CREEP TO RUPTURE BEHAVIOR OF CONCRETE BEAMS

BY

JOHN LEONARD WALKINSHAW
Diplome E.T.S. Geneva (Switzerland)
(1967)

Submitted in partial fulfillment

of the requirements for the degree of

Master of Science in Civil Engineering

at the

Massachusetts Institute of Technology

(February, 1969)

Signature of Author .....
Department of Civil Engineering, (January 20, 1969)

Certified by .....
Thesis Supervisor

Accepted by .....
Chairman, Departmental Committee on Graduate Students

ABSTRACT

CREEP TO RUPTURE BEHAVIOR OF CONCRETE BEAMS

by

JOHN LEONARD WALKINSHAW

Submitted to the Department of Civil Engineering on January 24, 1969 in partial fulfillment of the requirements for the degree of Master of Science in Civil Engineering.

A laboratory technique utilizing cast notched beams of cement paste, mortar and concrete was used to study the role of solid inclusions in the bending behavior of concrete. To determine the properties of the individual mixes, a series of conventional tests were made. The fracture parameters of the mixes were calculated. The long term behavior of the beams under loads approaching the ultimate was then established.

The results of this study show that most of the characteristics of the material improve when aggregate is present in the mix. In long term loading the service life of the beams increased with decreasing loads. At comparable ultimate load fractions (load levels) the creep rates were approximately the same. There was an apparent linear relationship (on semi log scale) between the maximum time to failure and the load levels tested. All three mixes showed lower stiffness after being subjected to load than if no load had been applied over the same period of time.

For the series of beams tested the long term ultimate strength was .80 of the short time static strength.

Thesis Supervisor: Fred Moavenzadeh

Title: Associate Professor of Civil Engineering

ACKNOWLEDGMENTS

The author wishes to thank Dr. Fred Moavenzadeh, thesis supervisor, for his careful review and positive suggestions during the preparation of this thesis. He further wants to acknowledge Mr. Arthur Rudolph for his help in the design and manufacture of the equipment and Mr. Ted Bremner for his valuable advice on certain sections of this thesis. Final thanks are extended to my other colleagues for their constant support throughout the project and to my wife for her patience and her typing of the drafts.

CONTENTS

CONTENTS

(continued)

LIST OF FIGURES

LIST OF TABLES

I. INTRODUCTION

Concrete when subjected to sustained loading has exhibited creep phenomenon. This phenomenon has long been recognized by structural engineers and several methods are suggested in the literature to account for creep behavior of concrete in the design of structural elements. The materials engineers on the other hand have been concerned with the understanding of the creep mechanism of concrete and have attempted to control the creep ratio through control of concrete proportion and quality of its constituents.

The creep behavior of concrete has mostly been considered at low levels of stresses and little is known about the behavior of concrete under sustained load levels close to its short time ultimate strength. This behavior which in other materials is referred to as static fatigue or creep to rupture is not only of interest in the design of structures but is also useful in the understanding of the behavior of material.

It is therefore the purpose of this thesis to obtain better understanding of the behavior of concrete in bending at load levels approaching the short time ultimate strength.

To study the influence of the different constituents of the concrete, cement, mortar and concrete beams were made. Fracture mechanics parameters were determined experimentally for each mix to explain what role solid inclusions play in the strengthening and toughening of concrete when subjected to the above loading conditions. Since failure occurs at the high levels of testing loads, relationships between load levels and time to failure were recorded. From these recordings the long term ultimate strength was determined and compared to that found in the literature for compressive strengths of the materials.

II. REVIEW OF LITERATURE

A review of the literature on creep and creep rupture of structural materials is presented in this section. The creep process and its basic causes in various materials are discussed in the hope that the progress made in other materials can be of use in the study of the behavior of concrete.

General Considerations of Creep to Rupture

In design for creep the most important properties used are creep strength and creep rupture strength. The American Society for Testing and Materials (ASTM) defines these properties as the highest stresses that a material can stand for a specified length of time without excessive deformation or rupture respectively [1]*.

As opposed to a cyclic fatigue test [2], which determines the number of cycles a material can safely endure over a certain stress range in an environment, a creep to rupture test [3] determines the service life under constant load or stress in the environment of application.

---

* Numbers in [ ] refer to references.

There are two principal methods for predicting creep strength:

1. Several specimens are tested simultaneously at different stresses and at the expected operating temperature. Time to reach the allowable strain is recorded for each specimen and a plot of stress vs. time can be drawn. From this plot, the service life of a specimen can be determined knowing the stress and temperature during operation.

2. The second method is based on the creep rate of the secondary (steady) creep. Knowing the allowable strain ε_1, the elastic strain ε_o, and the service life t_1, these can be combined to give an allowable minimum creep rate

$$V_o = \frac{\varepsilon_1 - \varepsilon_o}{t_1} .$$

This assumes transient creep to be completed and represents a schematic creep curve (Figure 1).

Each test is performed at different stress until the minimum creep rate appears to be well established. The results are plotted with V_o as a function of stress.

The creep to rupture concept is applied mostly to metals and polymers which have been playing an increasing role in modern technology. For example space technology and precision work require the exact knowledge of the material's behavior under increasingly high stresses and

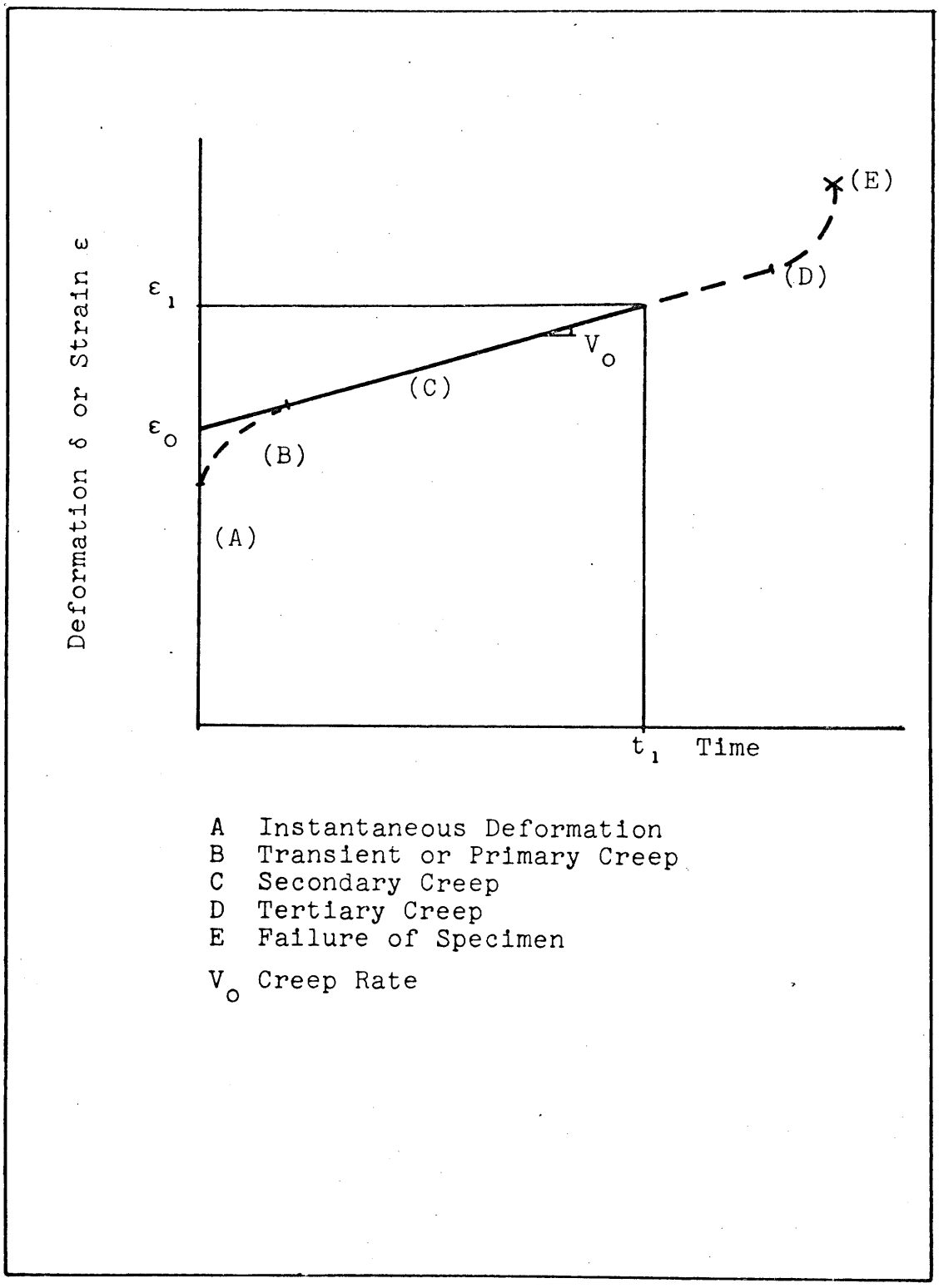

Figure 1. Schematic Creep Curve

temperatures. For metallic materials the time-dependent deformation and rupture characteristics become of primary concern at temperatures in excess of one-half of their absolute melting temperatures (.5 TM).

But in many new alloys the amount of creep deformation may not be the only factor governing service lifetime. Some have been found to fracture after very limited deformation, so time to rupture may be shorter than the time to reach a critical strain [4]. To understand the mechanisms of creep in these materials it is necessary to take a look at their microscopic structure.

The grain size in metallic materials has been shown to have a moderate effect on steady state creep [5,6]. In general, the creep rate decreases with increasing grain size, but in coarse grained materials ($2r > 0.1$ mm) the reverse can be true. But the grain boundaries transverse to the applied stress tend to be sites for void nucleation. This mechanism and energy considerations of fracture by vacancy creep are reviewed in detail by Cottrell [7].

Metallic materials also work-harden in the process of deformation and thus the creep rate results from a balance of simultaneous work-hardening and recovery processes. In the individual crystals two significant stress aided and thermally activated recovery processes exist. These are

cross-slip and dislocation climb [8,9] which both act primarily at different temperatures.

At low temperatures cross-slip prevails and is the movement of screw dislocations around obstacles. Recovery at high temperatures (above .5 TM) is done by dislocation climb. Climb is controlled by the rate of diffusion of vacancies to or from dislocation jogs under the action of the local stress fields.

Another method to reduce creep in metals is to alloy them with suitable elements. This raises the temperature of recrystallization and produces precipitants along the grain boundaries which reduces dislocation movements. Other mechanisms are also involved in creep of metallic materials. However it is not the scope of this review to go into further detail but to present a few mechanisms that are somewhat similar to those found in concrete.

In polymeric materials the trends are also similar to those of concrete and metallic materials. Many polymers exhibit fatigue or endurance limits in their stress vs. number of cycles (S-N) curves. The fatigue limit is often between 20% and 35% of the static tensile strength.

The fatigue life of a polymer is generally reduced by an increase in temperature. For example, the fatigue life of poly methyl methacylate (PMMA) decreases by 58% in going

from -30°F to 80°F [10]. These temperatures are below its glass transition temperature (90°F).

With the increasing wide use of polymers in everyday objects (plastic raincoats to rubber tires) it was found necessary to investigate the material properties under constant load (raincoat hanging on a hook, car in parking).

The creep mechanics in polymers for the steady state creep is viscous flow of the polymer chains around each other. A study done at Massachusetts Institute of Technology [11] on PMMA in creep to rupture shows that the stress limit (at 10000 hrs) is 35% of the short term (10 sec) static stress at room temperature. This limit varied with varying surface treatments, temperature and preheating of the specimens before testing.

The addition of fillers or glass fibers to the polymers increased the creep resistance by increasing the viscosity or basically following the same principles applied to metallic materials.

These trends of varying testing conditions are generally valid for the majority of the polymers and are widely covered in the literature and many references to them can be found in the books by Nielson [12] and Baer [13].

As for the work on concrete, it has been widely covered throughout this century.

Because of the wide variety of constituents entering a concrete mix it is often difficult to make definite comparisons, but general trends have been established and are well known. Most of the work has been done in either cyclic fatigue or creep at low levels of stress.

The cyclic fatigue testing simulates the loading of a wide variety of concrete structures the most important of which are bridges. Most studies have been done in compression and flexure although tests in tension and torsion are also reported.

The S-N (stress vs. number of cycles) curve for concrete does not exhibit a fatigue limit but continues to drop as N increases. For a large number of cycles (2×10^6), the cyclic fatigue strength in compression is approximately 50% to 60% of the short static strength. In flexural tension stress in nonreinforced beams, the "fatigue limit" has been reported [14] to be 55% for 2×10^6 cycles and between 40% to 66% of static strength for 10^7 cycles [15]. The mechanisms of failure occurring during the cyclic testing have been found to be strongly related to the following four parameters:

1. The presence of stress regardless of origin or time variation.
2. The repeating nature of some stresses.

3. The presence of discontinuities such as microcracks, macrocracks and structural heterogeneity.

4. The resistance of concrete to failure.

This last parameter has been defined by the following mechanism.

The internal flaws in a concrete specimen are large compared to the gel structure of the matrix. These flaws act as stress raisers. The average stress across the cross-section is much smaller than the stress at crack tips (Griffith theory). Microcracks relieve the stress at the tip of the macrocracks by the formation of new surfaces (expended surface energy) and the ability of the microcracks to stabilize macrocracks in a stress field is the resistance of concrete to failure.

The repeating stresses in cyclic fatigue modify the formation of microcracks and cause a slow, stable growth of macrocracks until the unstable condition is reached.

The other widely performed experiment is creep of concrete under constant stress. As seen previously in metals and other crystalline materials, creep is attributed to slip in crystals. While slip of this nature undoubtedly occurs [17] in aggregate particles and within crystalline particles that are part of hydrated paste, there is ample evidence that they are only secondary factors in creep of

concrete. Crystalline slip is normally detectable only above some threshold level of stress.

Creep of concrete has been observed at all stresses as low as 1% of ultimate [18]. It has been explained by many mechanisms of which the following or any combination of them are the most important:

1. Seepage of colloidal (absorbed) water from the gel formed by hydration of cement [19,20].
2. The effect of shrinkage [21,22].
3. The accessibility to water of the large internal surface of the gel structure [17].
4. Delayed elasticity [23].
5. Opening or closing of internal voids.
6. Intercrystalline deformation.

Some evidence supporting the first three mechanisms is that no creep was observed in tests made on dried pastes [24].

Creep of concrete is a linear function of stress up to 20% to 25% [25] or 35% to 40% of ultimate [17] depending on the authors. In either case this is in the normal working range of concrete in structures. A wide variety of research has been performed on creep in this range, studying the different behaviors and factors influencing such behaviors of plain and reinforced concrete. A fairly complete review on laboratory and field tests covering the years 1905-1956 can be found in Reference [26].

More recently creep behavior has been studied with the help of models. This enables researchers to formulate mathematical theories in the prediction of concrete deformation under load [25,27,28].

These models supplemented by laboratory tests allow also the computation of deformations of structures subjected to variable stress from results under constant stress [29]. Reference [29] explains three methods for doing this analysis. Each one of the three methods has a certain advantage in particular circumstances depending on the stress variation, the extent of creep data available and the accuracy desired.

Although most of the creep tests are performed in compression, some studies have been made in tension [26]. In tension, the rate of creep is greater in the first few weeks than in compression when reduced to 1 psi. Later the reverse is true but the ultimate is approximately the same. This finding stimulated the researchers to study creep in bending.

Their report on bending of nonreinforced beams subjected to a constant bending moment showed that the early creep of the fiber in the tension side was also greater than the corresponding creep of the compression side. Apart from these tests conducted at the normal working loads some researchers have studied the effects of higher

stress magnitudes.

The tendency to part from the exact proportionality increases as the values of the sustained stress increase [30]. Sustained stress above normal working stress produces creep that increases at progressively faster rate, as the magnitude of sustained stress is increased. Glanville and Thomas [31] proposed that a master curve could be obtained, for stresses up to 84%, by multiplying the strain at each load level by respective constants. These constants decreased with increasing load level (master curve at 84% of ultimate). They therefore concluded that "the mechanism of large deformations as failure is approached is the same as that of the creep at working stresses". This is stated to be false by many other researchers because generally failure has been recorded at lower stress levels than the ones quoted above. It is generally agreed that the ultimate strength under sustained loads determined on prismatical specimens is about 70% to 75% of the short time ultimate cube strength [14,32,33]. The performance of the concrete at this stress level is basically different from creep.

In the last ten years, the increasing interest in the actual fracture process of concrete has lead researchers to investigate these high levels of stress. Usually these tests are of short duration and involve a substantial

amount of electronic equipment.

Leslie and Cheesman [34] in measurements of the variance of the sonic velocity in a specimen noticed a marked decrease in it when the load approached 75% of the utlimate. Shah and Chandra [35] measured an increase in Poisson's ratio accompanied by an increase of cracking noises at the same load level as in [34]. These cracking noises were also observed in experiments by Rusch [36]. The detection of these cracking noises was first made at load levels between 30% and 50% of the ultimate and were intermittent up to 70% to 75% at which point they increased substantially.

Visual detection of the cracking in concrete was also undertaken by several researchers. Hsu [52] used a technique of first loading a small cylinder to a certain load level, unloading it, slicing it in thin sections, then ink staining the surface for visual observation of the crack patterns under a microscope. The first increase of bond cracks was observed at load levels above 30% of the ultimate and occurred around the larger aggregate (weaker bond strength). As the loading increased so did the number of cracks until they formed continuous crack patterns at 70% to 90% of the ultimate. This corresponds well with the findings using the sonic methods and accounts for the increase of Poisson's ratio. Hansen [33] used a different

technique, in as much as he cut slabs from prismatical specimens before drying and testing them. The specimens were loaded to certain levels and kept under constant stress until crack propagation had stabilized (4 days). The stress was then increased to a higher level and maintained again, and this process continued up to failure. The observance of the crack propagation could be made directly and it was reported that never more than two cracks caused failure.

This type of testing simulates more accurately the type of loading (long term) a structural member may undergo and the observed cracking is less likely to be due to experimental procedure (machining).

Another method of showing the cracking of concrete at high levels was presented by Glucklich [53] in 1959. Two series of specimens were tested, one in a normal "hard" machine and the second with the interpositioning of a spring between the specimen and the crosshead to make a "soft" machine. The specimens tested in the "soft" machine all failed at lower loads than in the "hard" machine.

The essential difference between the two types of loading consists in stored energy considerations. In the "soft" machine there is a practically unlimited store of elastic energy available whereas in the "hard" machine the

only energy available is stored in the specimen. As seen previously, the mechanism of fracture of the material, in a "hard" machine, is such that local fracture is usually arrested soon after it starts spreading because its energy supply is exhausted. In the "soft" machine, when crack growth was checked by a region of low energy, the spring contributed an additional supply of energy to overcome the obstacle and produced earlier failure of the specimen.

This method of testing in a "soft" machine is nearly the equivalent of testing a specimen to failure by providing constant stress and Glucklich's conclusions were: "Concrete is sensitive to static fatigue. The conclusion is therefore that in strictly sustained loads or in statically determinate systems, the time effect on strength can lead to total failure at loads below the normal breaking loads....."

Therefore the failure load of concrete could be defined as the load at which fast crack propagation begins.

In the next sections it will be explained how, in this study, the failure loads were determined for cement paste, mortar and concrete beams in bending. Fracture mechanics parameters and other material properties will also be discussed.

III. MATERIALS AND PROCEDURE

In this section the materials and the test procedures used to determine the results are discussed.

Materials

The sand and gravel (pea stone) used in the different mixes were obtained from a local supplier. The conventional tests and gradation results are presented in Tables 1 and 2.

The aggregates were oven dried and stored in containers in the laboratory. After the first gradation tests, it was decided to exclude the sand retained on the Number 4 sieve (approximately 6%) to correspond more accurately to the Bureau of Reclamation Specifications [40]. Also the gravel retained on the 3/8" sieve (approximately 24%) was excluded because of the maximum size restrictions [41] for the specimen geometry described later. The cement used was Type 1 Portland Cement. The manufacturer's laboratory report for this cement is shown in Table 3.

Table 1

Results of Conventional Tests on the Aggregates

Origin: uncrushed extracted from piles

Sand:

Specific Gravity SSD	2.63
Unit Weight (oven dry)	111 lb/ft^3 (1.78 g/cm^3)
Moisture Content SSD	1%
Fineness Modulus	2.75
Maximum Size ϕ	.187 in (0.45 cm)

Gravel:

Specific Gravity SSD	2.67
Unit Weight (oven dry)	96 lb/ft^3 (1.54 g/cm^3)
Moisture Content SSD	1%
Fineness Modulus	5.60
Maximum Size ϕ	.375 in (0.95 cm)

Table 2

Gradation of Aggregates

Sand:

% rounded to nearest whole number

Sieve Size	Retained on Sieve (% by weight)	Cumulative (% by weight)	Bureau of Reclamation Specification
No.4	0	0	0- 5
8	16	16	10-20
16	17	33	20-40
30	19	52	40-70
50	27	79	70-88
100	16	95	92-98
		275	

Fineness Modulus 275/100 = 2.75

Gravel: (pea stone)

Sieve Size	Retained on Sieve	Cumulative
3/8"	0	0
1/4"	71	71
No.8	22	93
16	6	99
30		99
50		99
100		99
		560

Fineness Modulus 560/100 = 5.60

Table 3

Manufacturer's Laboratory Report
on the Portland Cement

Specification and Type: Type I Bag

CHEMICAL

SiO_2	20.39%
Al_2O_3	6.20%
Fe_2O_3	2.69%
CaO	63.36%
MgO	3.20%
SO_3	2.22%
Ignition Loss	0.36%
Insoluble Residue	0.09%
Potential Compounds	
Tricalcium Silicate	51.09%
Tricalcium Aluminate	11.88%

PHYSICAL

Wagner	1962
Blaine	3321
Autoclave Expansion	0.431%
Time of Setting, Gillmore	
Initial (hr:min)	3:13
Final (hr:min)	5:02
Compressive Strength, psi	
1-day	1700
3-day	3500
7-day	4880
28-day	5768
Air Entrainment, % by volume	9.3%

Specimen Size

A notched beam subjected to three point bending was selected as the type of specimen for use in this study of creep to rupture of concrete for several reasons. Notching of the specimen on the tension side creates a high stress concentration on a relatively small region. The location of fracture initiation is thereby controlled. It also reduces the scatter in the ultimate load bearing capacity. Testing the concrete in a tensile fashion focuses on the weakest and the microscopically most likely mode of fracture.

The nominal dimensions of all the beams were 2" x 2" x 22". All the specimens had notches such that the ratio of notch depth to overall depth a/d was .375 (see Figure 2).

The notch geometry was designed for easy removal of the beam from the mold (see Figure 3). The notch could be removed from the mold partitions if unnotched beams were desired. The notches were situated at the midspan on the tensile faces of the specimen and were made of brass.

Design of Mixes

Trial mixes were made to determine the best water-cement ratio (W/c) and aggregate-cement ratio (A/c) to

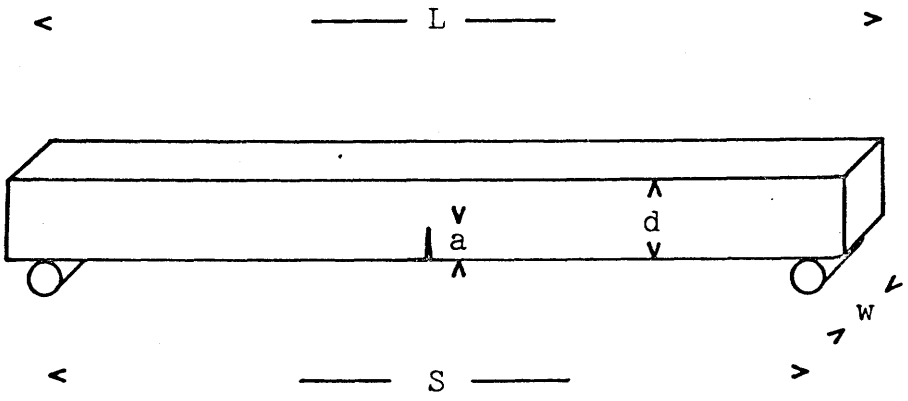

Notch Depth	a =	.75"
Beam Depth	d =	2"
Beam Width	w =	2"
Overall Length	L =	22"
Span	S =	20"

a/d = .375

S/d = 10

Figure 2. Beam Geometry

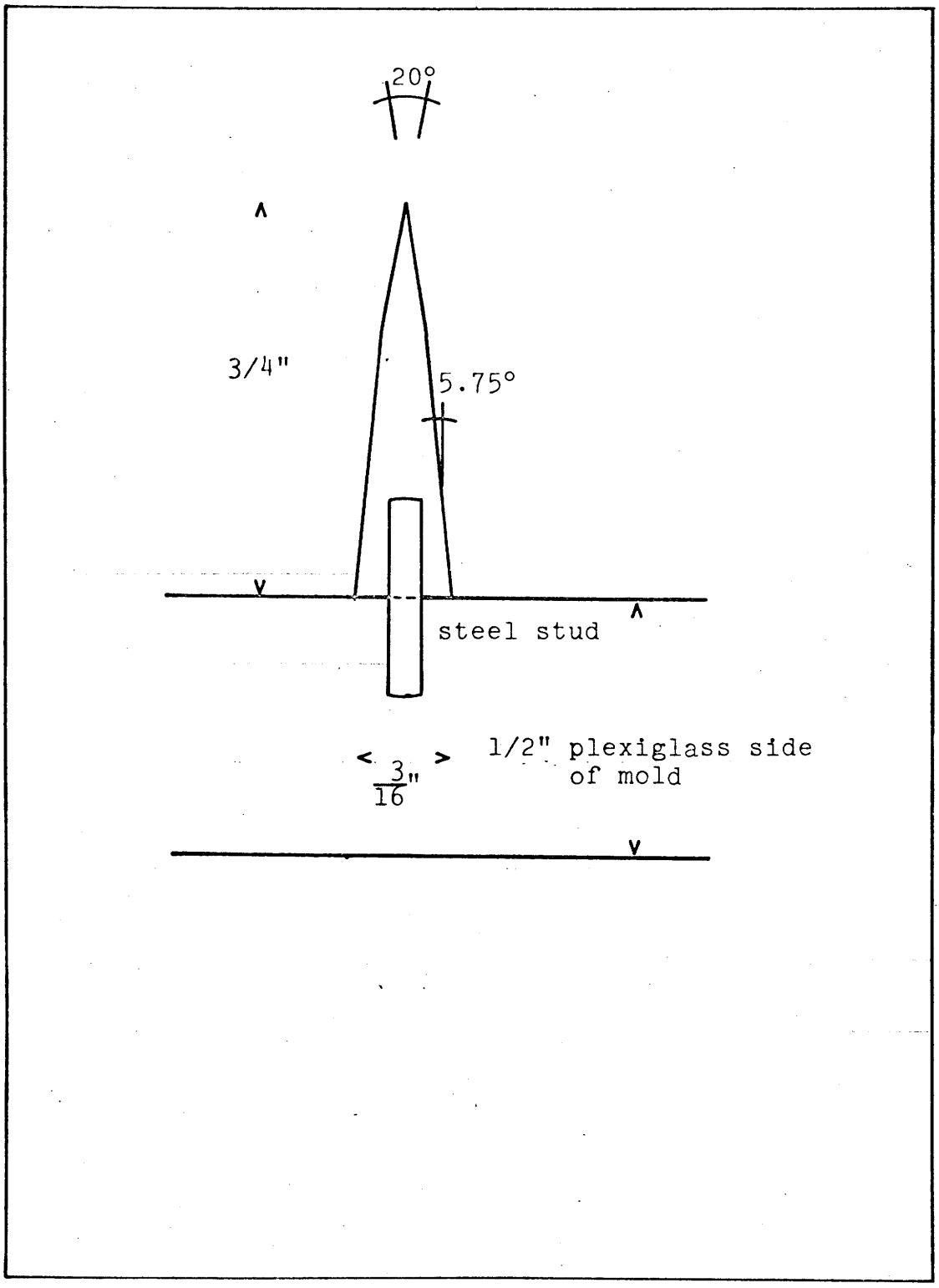

Figure 3. Geometry of the Removable Brass Notch

obtain workable mixes. It was felt that an A/c ratio lower than 3.0 would not be representative of a practical mix. Also the W/c ratio of .4 was found to be the maximum ratio that could be used in cement paste without excessive bleeding. Higher A/c ratios than 3.0 were tried but the mixes could not be satisfactorily molded.

The proportions by weight of the final mixes are presented in Table 4. The weights of the aggregates are given in the saturated surface dry (SSD) condition.

Fabrication and Curing

Each batch (approximately 100 lbs) was prepared to make twelve beams cast into two plexiglass molds. The molds and notches were oiled prior to each pouring.

The aggregate, water and cement were preweighed taking into account that the aggregate was not in SSD condition. A one cubic foot capacity concrete mixer was used and mixing was continued for five to six minutes after all the mix constituents had been added. The mix was then poured in the molds in three layers and the vibrating table on which the mold was resting was activated two to three minutes for each layer put in.

Following the casting of the twelve beams the molds were covered under polystyrene sheeting. Saturated sponges

Table 4

Mix Proportions

	Cement Paste	Mortar	Concrete
water/cement	.4	.4	.4
sand/cement		3.0	1.2
gravel/cement			1.8
aggregate/cement		3.0	3.0
unit weight g/cm^3	2.04	2.34	2.43
unit weight lb/ft^3	128	146	152
cement content $bags/yd^3$	26	10	10

were placed under the sheeting to insure a high humidity curing prior to demolding.

The beams were demolded after twenty-four hours, numbered, dated and cured in water until testing at twenty-eight days.

Testing Equipment and Testing Procedure

Static Tests: The static tests were performed on an Instron Universal Testing Machine. The load cell used had a maximum capacity of 10000 lbs and the span of the beam was 20 in. This testing arrangement can be seen in Figure 4. Initially, certain standard flexure tests had to be performed on the three mixes before the creep to rupture testing could begin. To determine the crosshead rate which would meet the ASTM standards [42], twenty-four beams were cast of each mix, half of which were unnotched. These beams were tested at both seven days and twenty-eight days at two different crosshead rates. It was found that the rate of .005 in/min could be used and it is at this rate that all the subsequent ultimate load determinations were made.

Creep to Rupture Tests: In this study two types of loading devices were used for the long term loading of the notched beams. In the first device, shown in Figure 5, it was possible to record the deflection of the beam by means

Figure 4. Instron Testing Machine with Beam Set-up

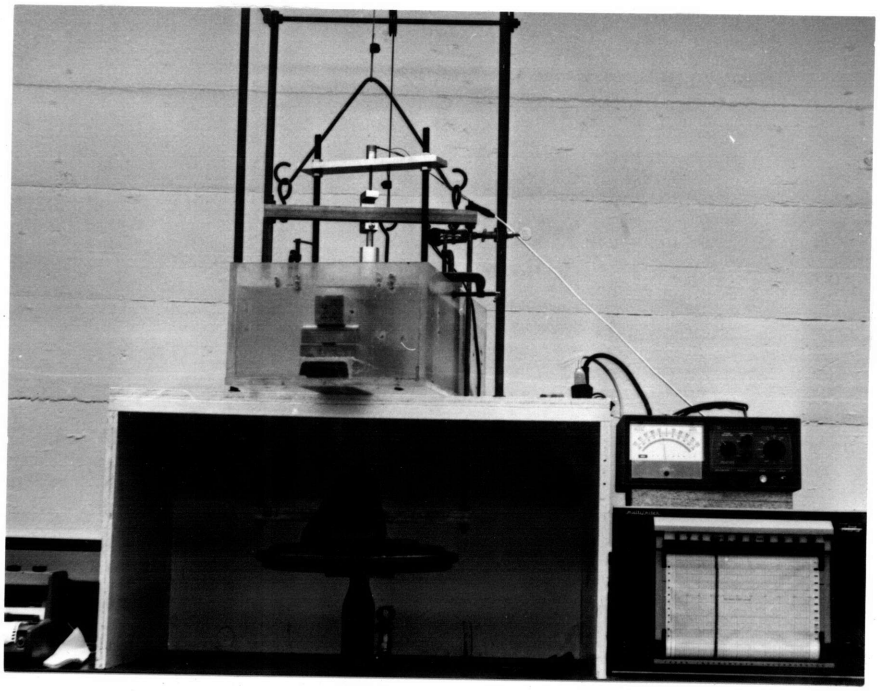

Figure 5. Creep to Rupture Loading Device with Recorder

of an LVDT Transducer. The full scale on the chart paper (100 divisions) was calibrated to be .02 in. The recorder had two chart speeds: 1 in/min used in the first minutes of the test and 2 in/hr used until the end of the test. In tests of expected short duration the recorder was left on 1 in/min.

The other loading device is shown in Figures 6a and 6b. Six of these devices were made so that a total of seven beams could be tested at one time. In this second loading device the load is applied through a steel lever bar at each test position. The weight is applied at the end of the bar. The lever arm distances were such as to apply the load at the midpoint of the test specimen of twice the suspended weight. The weight of the bar was included in the applied load.

The timing at each loading position was accomplished with an electric calendar clock connected to a microswitch. Failure of the specimen released the lever arm and opened the microswitch, thereby stopping the clock. The time of day in which a failure occurred could be determined by advancing the hands of the clock to the next "12 o'clock" position and seeing if the calendar date changed.

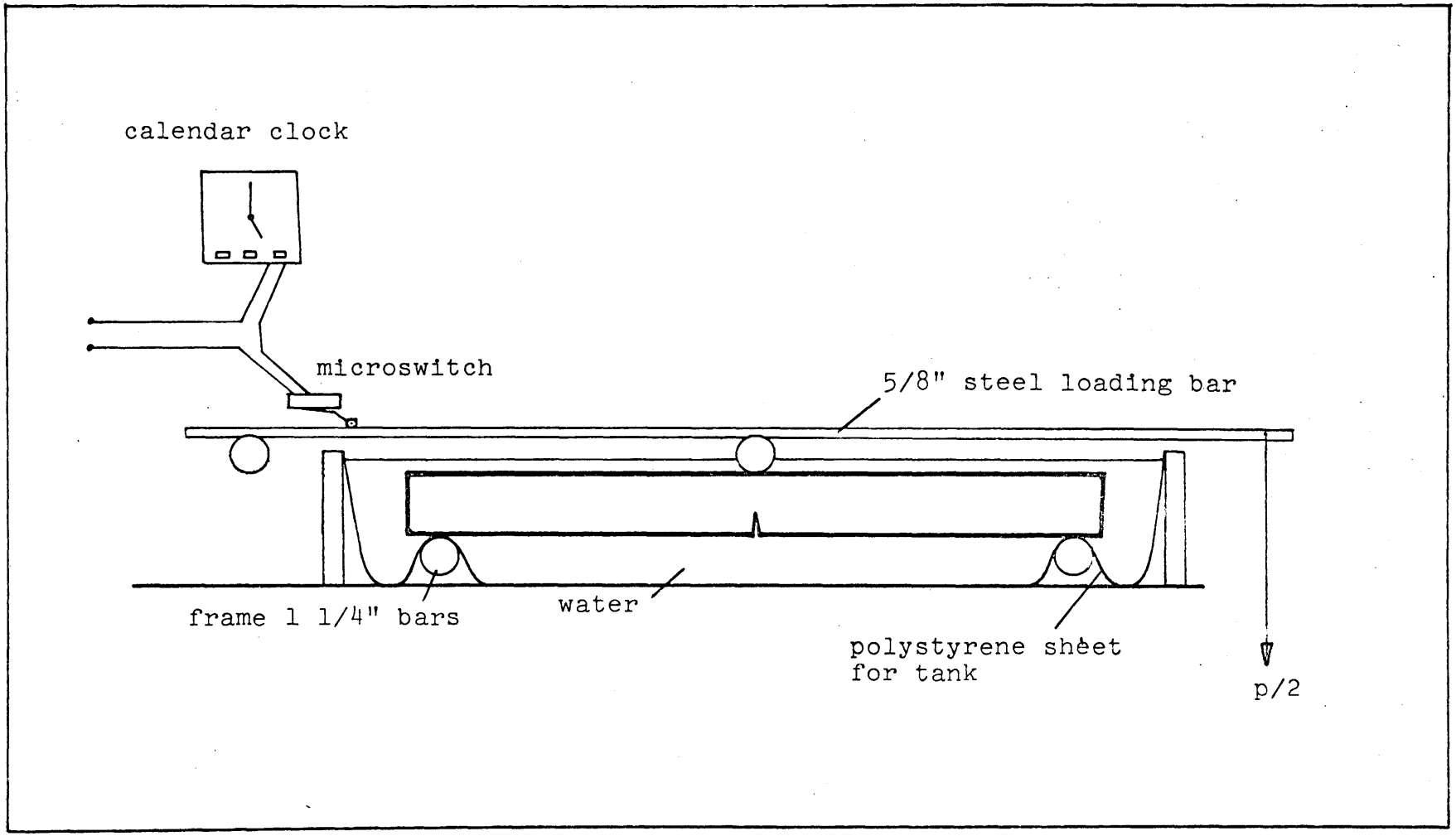

Figure 6. Creep to Rupture Loading Device with Clock

a) Schematic Representation

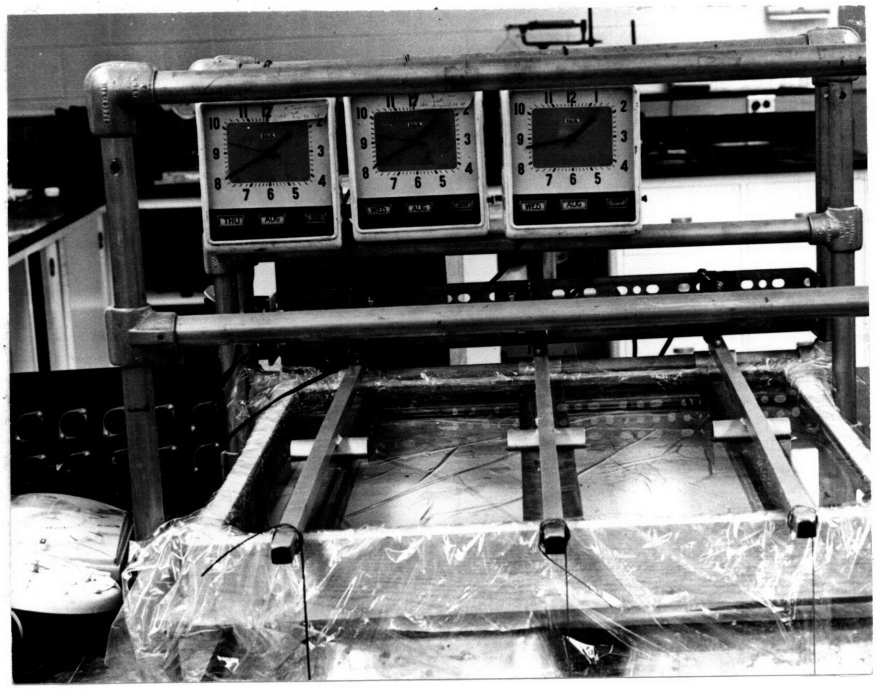

b. Actual Set-up

Figure 6. Creep to Rupture Loading Device with Clock

IV. RESULTS AND DISCUSSION OF RESULTS

In the first part of this section the results of the conventional tests, such as modulus of rupture, modulus of elasticity and compressive strength, performed on the three mixes are discussed.

In the second part the fracture mechanics parameters (critical stress intensity factor K_c , critical strain energy release rate G_c and the surface energy γ) are determined from tests on the notched beams for each mix.

In the final part of this section the results of the creep to rupture tests are discussed and compared with the trends noted in the other tests for paste, mortar and concrete.

Conventional Tests

Modulus of Rupture: The first property determined for each mix from the unnotched beams was the modulus of rupture [42]. The values computed for seven day and twenty-eight day tests are presented in Table 5. These values compare well with values presented by Walker and Bloem [44] if their values (in graph form) are extrapolated

Table 5

Modulus of Rupture in Flexure

(7 days & 28 days)

Age at Testing	7 days		28 days	
Loading Rate (in/min)	0.002	0.005	0.002	0.005
Paste	1050 -14%+19%	1085 -8%+10%	975 ±24%	1155 ±15%
Mortar	910 ±7%	920 ±3%	985 ±4%	1070 ±4%
Concrete	765 ±10%	820 ±10%	840 ±12%	935 ±2%

results in psi

for the richness* of mixes used in this study (Table 4).

Certain trends are noticeable in these results such as a decrease in the flexural strength with the change in aggregate size from mortar to concrete [54]. This can be explained by calculations of the characteristic flaw sizes of each mix [51]. They were shown to increase in size in the same proportion as the maximum aggregate size. The calculations were based on the assumption that the cracks were "penny shaped" in an infinite body subjected to uniform tension. Although this assumption is not exact for bending, the values calculated give a good explanation for the decrease in strength with increase of aggregate size. Another trend is the general increase of strength with increase of strain rate which is characteristic of concrete mixes and is well documented in the literature [20,42].

It was also noted during the testing of the beams that each mix had a characteristic mode of failure, especially noticeable on the notched beams (see Figure 7).

Cement paste was characterized by sudden catastrophic failure known as "unstable" fracture. This means that the energy stored in the specimen while loading (area under the curve) is in excess of that necessary to propagate a

---

* See section on "Design of Mixes".

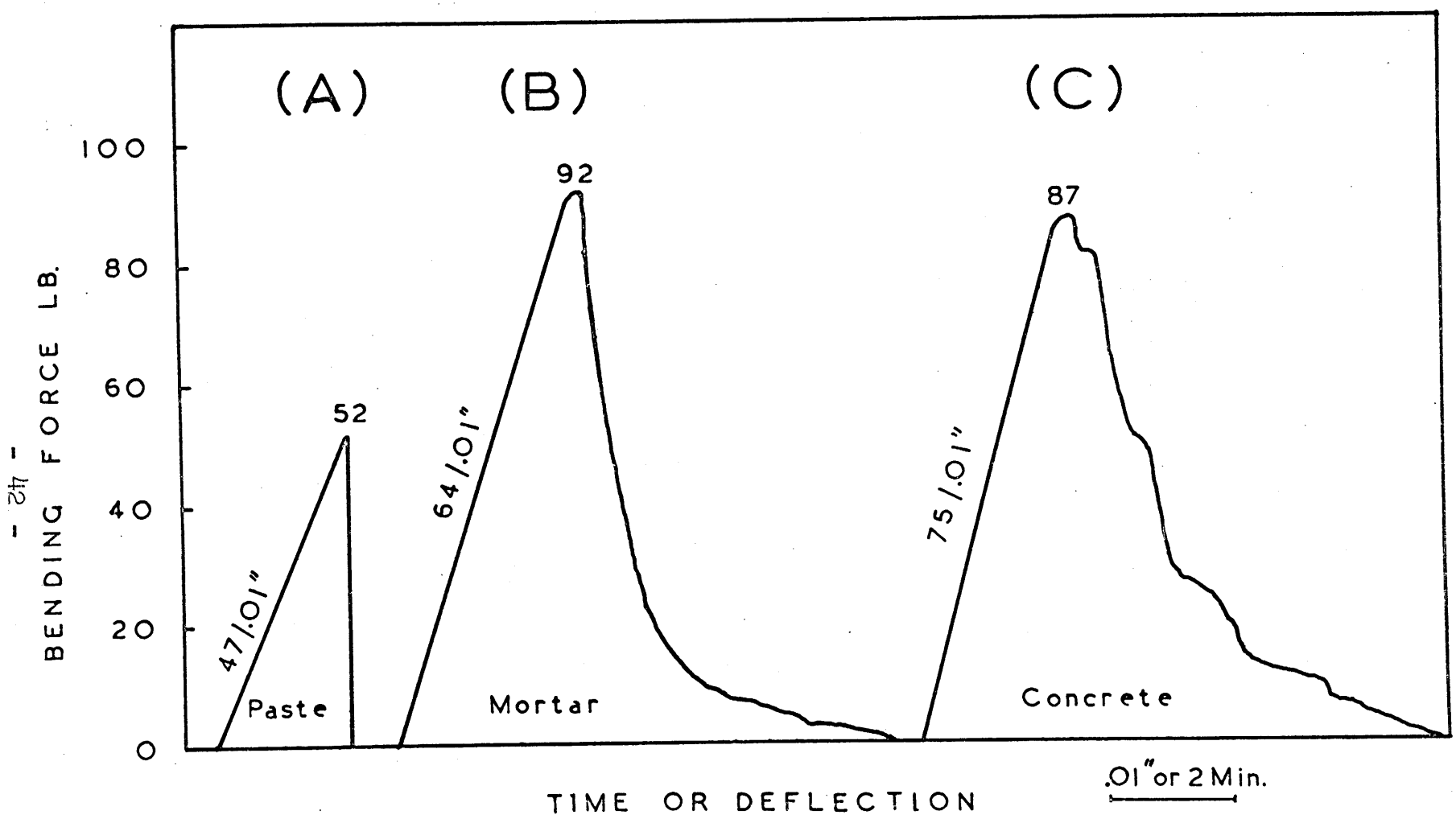

Figure 7. Typical Load-Deflection Curves Representing (A) Catastrophic, (B) Semi-Stable, (C) Stable Fracture

starting crack through the specimen. Once started, the crack propagates rapidly through the notched cross-section, leading to complete failure of the beam in a fraction of a second.

The failure of the mortar beams was what is known as "semi-stable" fracture. In this mode of fracture the energy stored in the specimen was not quite sufficient to drive the crack through the specimen. More energy had to be added to completely separate the two sections.

The third mode, represented by concrete, is "stable" fracture which means that the input of energy had to be increased continually to propagate the slow moving crack through the specimen cross-section. It is interesting to note the energy required to fracture the specimens increases with the increase of aggregate size (mortar vs. concrete), and this will be referred to in more detail in the "Fracture Mechanics Parameters" section.

Modulus of Elasticity: Values of the modulus of elasticity E were necessary to calculate the fracture mechanics parameters of the mixes used in this study. These values were first determined using the load-deformation curves obtained from flexure tests. These results are presented in Table 6. Since the values obtained in this manner are lower than expected for these types of

Table 6

Modulus of Elasticity
Determined from Flexure Tests

(7 days & 28 days)

	Modulus E x 10^6 psi			
Age at Testing	7 days		28 days	
Loading Rate (in/min)	0.002	0.005	0.002	0.005
Paste	.938	1.100	1.063	1.230
Mortar	1.450	1.225	1.250	1.620
Concrete	1.340	1.440	1.375	1.675

Modulus of elasticity E determined from

$$\delta = \frac{1}{48} \frac{PS^3}{EI}$$

where δ = maximum deflection of beams
P = maximum load
S = span of beam tested
E = modulus of elasticity of the material
I = moment of inertia of beam cross-section

mix [19]*, two other methods were used to determine E using mechanical strain gages. The first measurements were taken on the tension side of unnotched beams as shown in Figure 8a and 8b. Later, the same type of measurements were taken at one-hundred-fifty-four days on halved sections of notched beams (11 in) on a 10 in span. The results are plotted as stress-strain curves with the stress calculated at the level of the center of the gage point. Each curve presented in Figure 9 is the average of three tests, and show the same trends as those presented in [55].

The second measurements with the strain gage were performed on standard 2" x 4" cylinders tested in compression [43]. The strain values were recorded on opposite sides of the cylinders and were averaged for each stress level. The tests were performed at twenty-eight and one-hundred-forty days. The stress-strain curves presented in Figure 10 are the average of four measurements obtained on two cylinders. The values of the computed moduli and associated compressive strengths are presented

---

* Later measurements showed that 45% to 55% of total deformation was being absorbed in the supports. As no definite correcting factors could be calculated for each mix, the values of Table 6 are not modified.

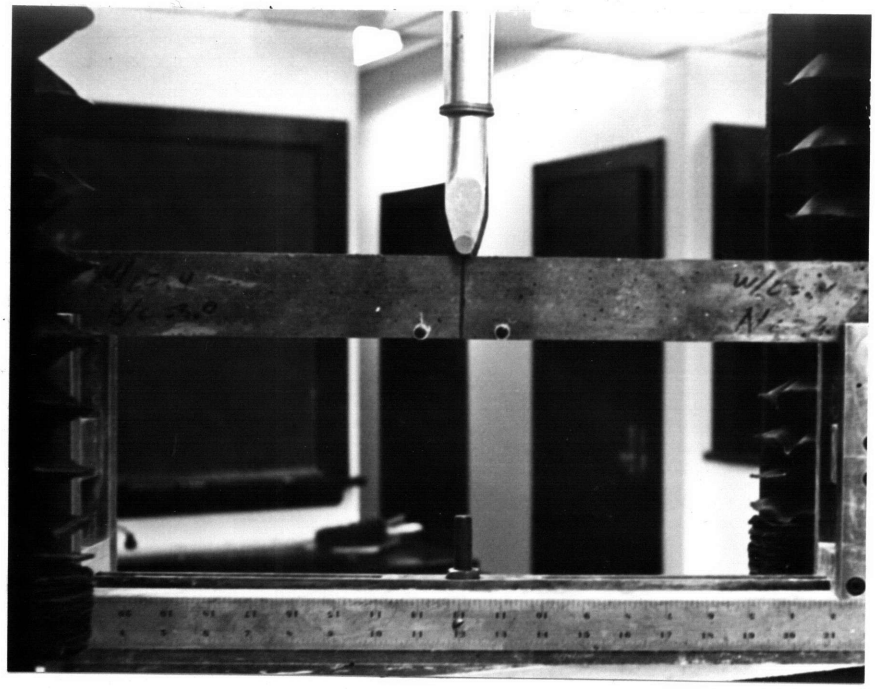

a. Position of Strain Gage Pins

Figure 8. Strain Measurement on Tension Side of Beams in Flexure

b. Positioning of Mechanical Strain Gage
1 Division: strain of 2.49×10^{-5}

Figure 8. Strain Measurement on Tension Side of Beams in Flexure

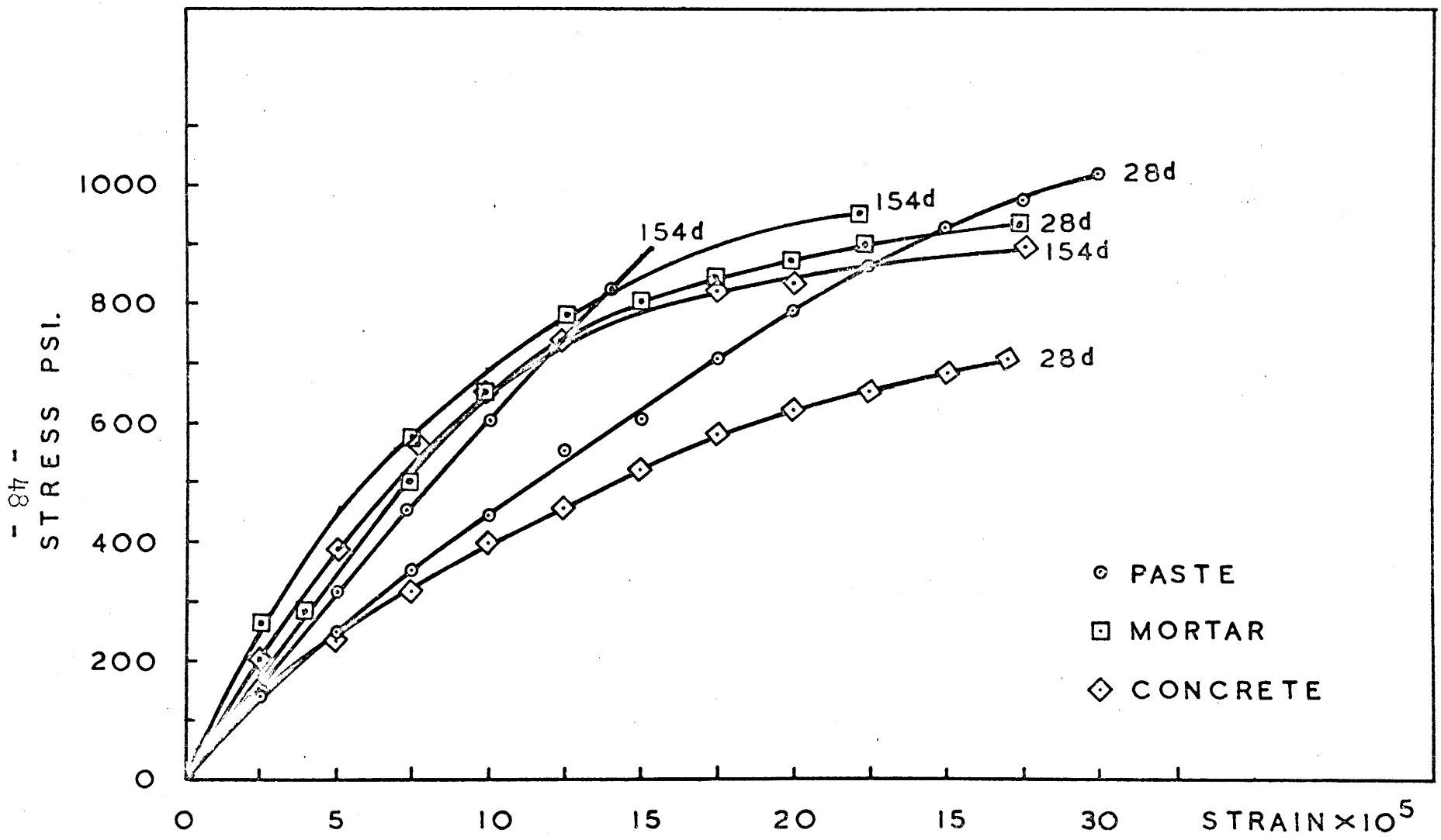

Figure 9. Stress-Strain Curves for Measurements on Tension Side of Beams in Flexure.

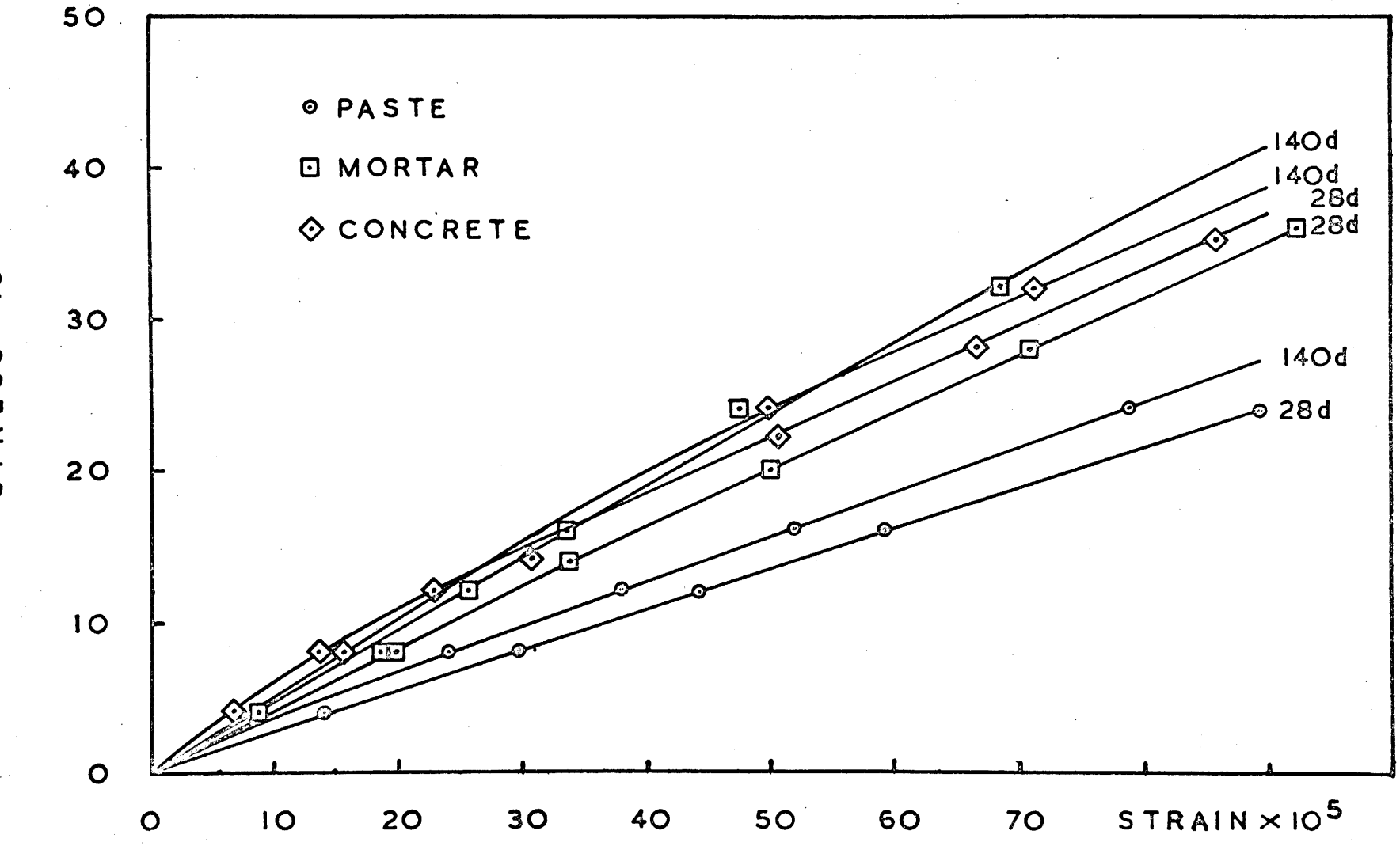

Figure 10. Stress-Strain Curves from Measurements on 2" x 4" Cylinders in Compression

in Table 7. This table also contains the compressive strengths of 2 in cubes tested at twenty-eight days.

As can be noted, discrepancies exist in the values of modulus of elasticity arrived at by the different methods of testing. Moduli as determined in compression were chosen to be used in calculation of fracture mechanics parameters for the following reasons:

1. The results of flexural tests were not accurate (see footnote, previous page).
2. The curvature of the stress-strain curves determined on the tension face of the beams, made it impractical to decide at which stress level E would be representative of each mix. This curvature was also noted in similar experiments by Welch [55].

The moduli as determined in compression correspond well with the results in References [44,45] for the aggregate size used and show the general trend of increase of E with increasing aggregate size. The presence or absence of aggregate (mortar vs. paste) appears to produce a greater change in modulus than a small change in aggregate size (mortar vs. concrete).

Compressive Strength: The third property determined was the compressive strength, from 2" x 4" cylinders and 2 in cubes. These values are presented in Table 7 and are

Table 7

Modulus of Elasticity and Compressive Strength
Determined on 2" x 4" Cylinders
(28 days and 140 days)

and

Compressive Strength of 2" Cubes
(28 days)

Age at Testing	28 days		140 days	
	Modulus E (psi)	Compressive Strength (psi)	Modulus E (psi)	Compressive Strength (psi)
Paste	2.68×10^6	7650 ± 4%	3.04×10^6	7100 $^{+\ 25\%}_{-\ 32\%}$
Mortar	3.97×10^6	6400 $^{+\ 6.5\%}_{-\ 15\%}$	4.75×10^6	7500 $^{+\ 15\%}_{-\ 17\%}$
Concrete	4.45×10^6	7100 $^{+\ 11\%}_{-\ 14\%}$	4.80×10^6	6540 $^{+\ 19\%}_{-\ 15\%}$

Secant modulus of elasticity calculated from the strain recorded at 2400 psi stress level.

The cylinders were capped at both ends with quick drying plaster of paris.

	Paste	Mortar	Concrete
Compressive Strength (psi)	7200 ± 4%	7700 $^{+\ 8\%}_{-\ 14\%}$	8300 ± 4%

for tests at twenty-eight days and one-hundred-forty days on the cylinders and only twenty-eight days for the cubes. As it can be noted the general values are within the expected range for these types of mixes (10 bags/yd^3).

No particular trend could be noted on the strengths of the cylinders, most likely because the values are taken from the same cylinders from which the moduli E were calculated. The measurements of E required cycling of the load a few times which may have reduced the strengths somewhat. However the testing of the 2 in cubes showed a general increase of strength with the increase of size of aggregate which is what is to be expected for this range of aggregate and specimen size [44].

Calculation of Fracture Mechanics Parameters

During the preliminary test of notched and unnotched beams (see "Testing Procedure") a series of the materials properties were determined. From the notched beams, the critical stress intensity factor K_c ,the critical strain energy release rate G_c , and the surface energy γ were calculated using the following relations.

---

* The applicability of these relations to concrete are discussed in detail in Reference [46].

The expression for determining K_c was taken from Reference [47] and is

$$K_c = Y \cdot a^{1/2} \cdot \frac{6M}{wd^2}$$

where: a = notch depth,
d = beam depth,
w = beam width,
M = applied bending moment,
Y = f(a/d) constant = 2.08.

This expression is very similar to that used by Lott and Kesler [48] in their study on fracture of concrete. The only difference is the value of the constant which changes the values by 6%.

Having calculated K_c, the values of G_c can be determined using Irwin's [49] expression for brittle fracture of materials

$$G_c = \frac{\pi K_c^2}{E}$$

where: E = modulus of elasticity of the material.

Subsequently γ_G can be determined from the expression

$$\gamma_G = \frac{G_c}{2}$$

where: γ_G = specific surface energy from

Irwin's expression, and specific surface energy = energy to fracture a specimen/total area of new surfaces created.

Another method for determining the surface energy γ [50] is based on the assumption that the energy expended to induce a stable fracture is equal to the surface energy of the newly formed surfaces. A measure of the energy input to fracture a beam is the area under the load-deflection curve. This is called the effective surface energy γ_{eff} if it is reduced to the energy required to break a unit cross-sectional area and is expressed as the following.

$$\gamma_{eff} = \frac{U}{2A}$$

where: U = measured input energy,
A = surface area of cross-section,
γ_{eff} = effective surface energy per unit area.

The values of these fracture parameters for cement paste, mortar and concrete are shown in Table 8. Each one is an average of three beams tested. The differences observed between the two measured surface energies γ_G and γ_{eff} are due to the following causes:

1. Cement paste beams fail unstably (see Figure 7); therefore, the measured input energy U is in excess of that needed to fracture the

Table 8

Fracture Mechanics Parameters
for Cement Paste, Mortar and Concrete

(28 days)

	k_c lb · in$^{-3/2}$	γ_G in · lb/in^2	γ_{eff} in · lb/in^2
Paste	357	0.075	0.084
Mortar	540	0.115	0.367
Concrete	516	0.094	0.386

Loading Rate = 0.002 in/min

	k_c lb · in$^{-3/2}$	γ_G in · lb/in^2	γ_{eff} in · lb/in^2
Paste	368	0.080	0.104
Mortar	550	0.108	0.388
Concrete	610	0.131	0.588

Loading Rate = 0.005 in/min

k_c = critical stress intensity factor

$\gamma_G = \pi k_c^2/2E$ Irwin's "effective" surface energy

γ_{eff} = effective surface energy

specimen. This results in a value of γ_{eff} which is slightly higher than γ_G calculated from G_c .

2. The large differences between γ_G and γ_{eff} for mortar and concrete are due to the fact that the surface area A used for determining γ_{eff} was taken as the nominal cross-section (2" x 1.25"). This assumes that the crack propagates in a straight line through the specimen and does not account for the new surfaces due to multiplicity of crack propagation. This phenomena is well documented in the literature and many studies have measured the extent of this discrepancy [33,35,39,48]. No such measurements were made in this study.

Comparing the different mixes for each method of measuring the surface energies it can be noted that it takes four or six times more effective energy γ_{eff} to fracture the mortar and concrete beams than it does to fracture the cement paste beams. This corresponds with the increased multiplicity of cracks with the increase of aggregate size. However, measurements of the surface energy using Irwin's theory do not produce the same pronounced trend of increasing surface energy with increasing size of aggregate. This is because the surface energy is related to the bond paste-aggregate and it is known that this bond weakens as the size of aggregate

increases [54]. So γ_G does not increase as markedly for the three mixes as does γ_{eff}. These values of the fracture mechanics parameters show the same trend as values published in Reference [46]. Generally the values were higher but the specimens tested in this study were also larger. It has been shown [51] that these parameters do increase with increase of specimen size, and general accordance can be claimed.

Creep to Rupture Tests

In order to study the gradual yielding of concrete subjected to high stresses the following procedure was adopted for each test batch. First, three specimens were randomly chosen from the batch and tested to determine their ultimate strength. During these tests load-deformation data was also recorded. The average value of the ultimate strengths recorded was then calculated. Load levels were then defined as fractions of this ultimate strength. A series of preliminary tests were conducted in order to determine the appropriate load levels to be used in this study. The load levels chosen were .80, .85 and .90 of the ultimate.

The beams were next placed in the previously described creep to rupture loading devices and subjected to the

desired load levels. Testing was terminated at rupture or when the desired creep data had been recorded.

The creep behavior as observed in this study is presented in Figures 11, 12 and 13 for cement paste, mortar and concrete respectively.*

The following parameters were chosen for comparing the characteristic behavior of the three mixes used in this study:

creep rates

magnitude of creep

tertiary creep

deflection at failure

effects of static fatigue on short time tests

Creep Rates: The creep rates recorded for each mix can be compared in two ways:

a) the rate obtained at each load level as shown in Figures 11, 12 and 13, and

b) the normalized creep rate, i.e. the creep rate divided by the corresponding load level.

Comparing the creep rates at each load level, a fair degree of uniformity was observed in the results** of paste

---

* A detailed presentation of the observed beam deflections data is contained in Appendix B.

** Except when failure occurred, there was no visible difference in creep rates for .80 and .85 load levels.

Figure 11. Creep to Rupture Recordings for Cement Paste

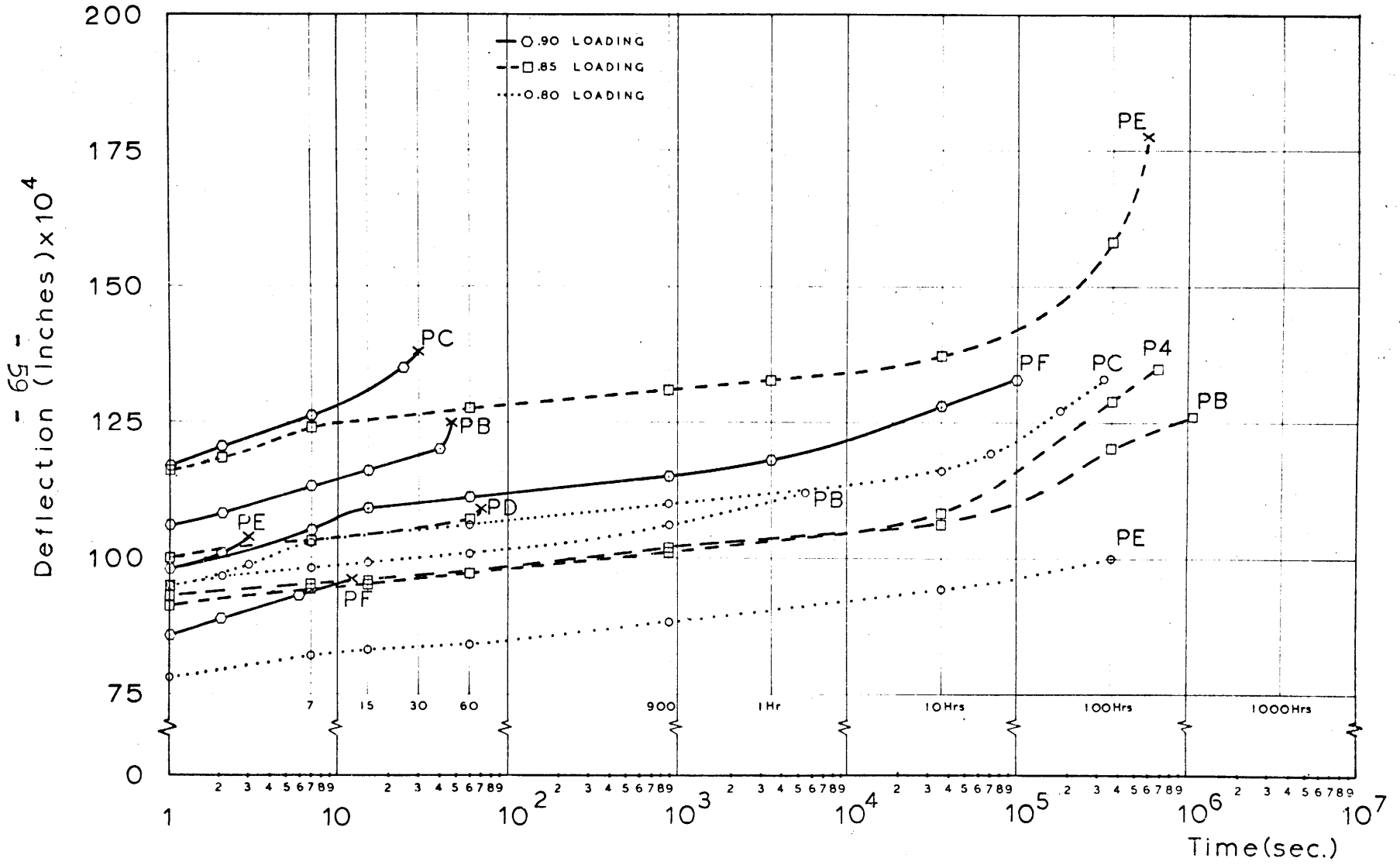

Figure 12. Creep to Rupture Recordings for Mortar

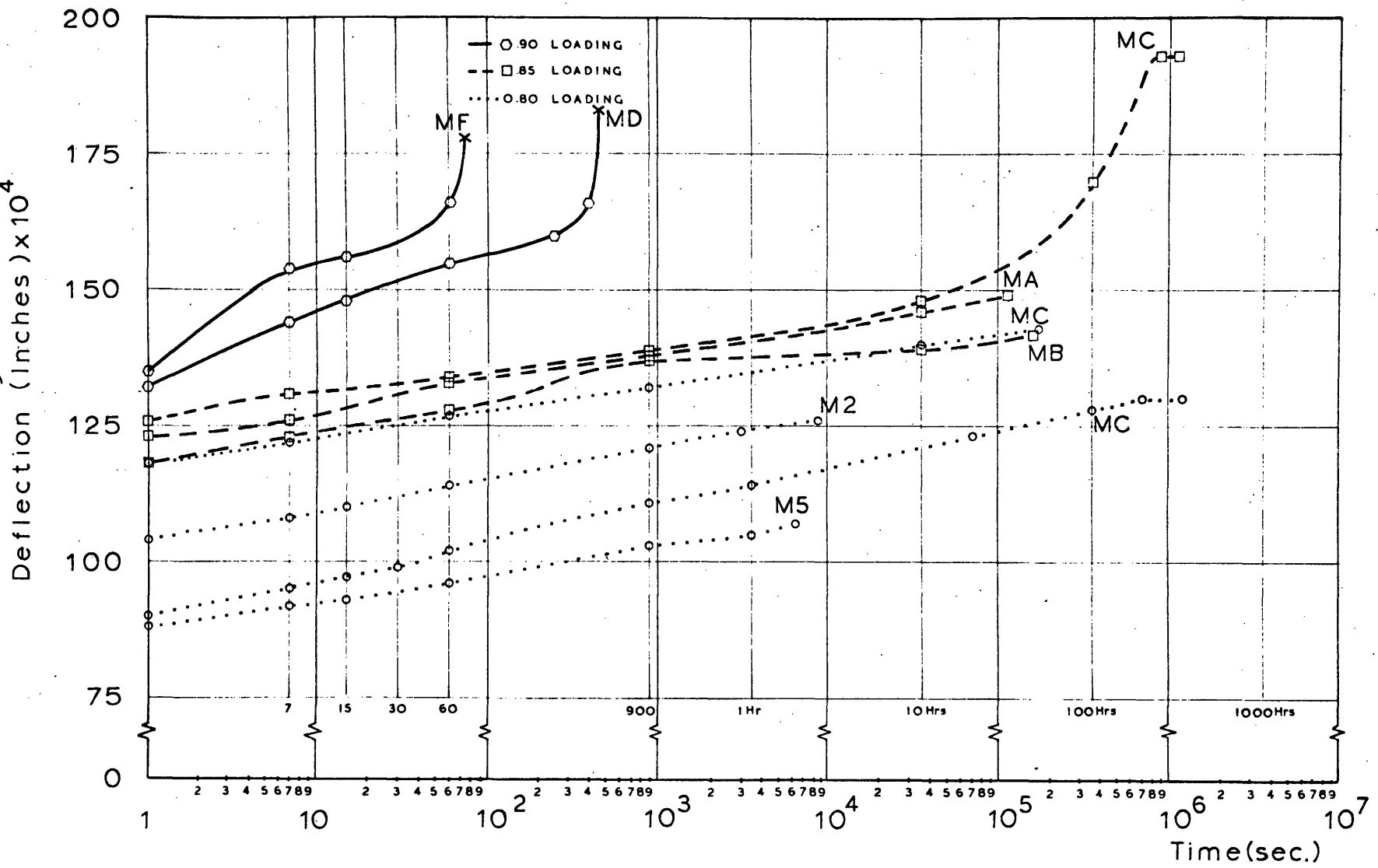

Figure 13. Creep to Rupture Recordings for Concrete

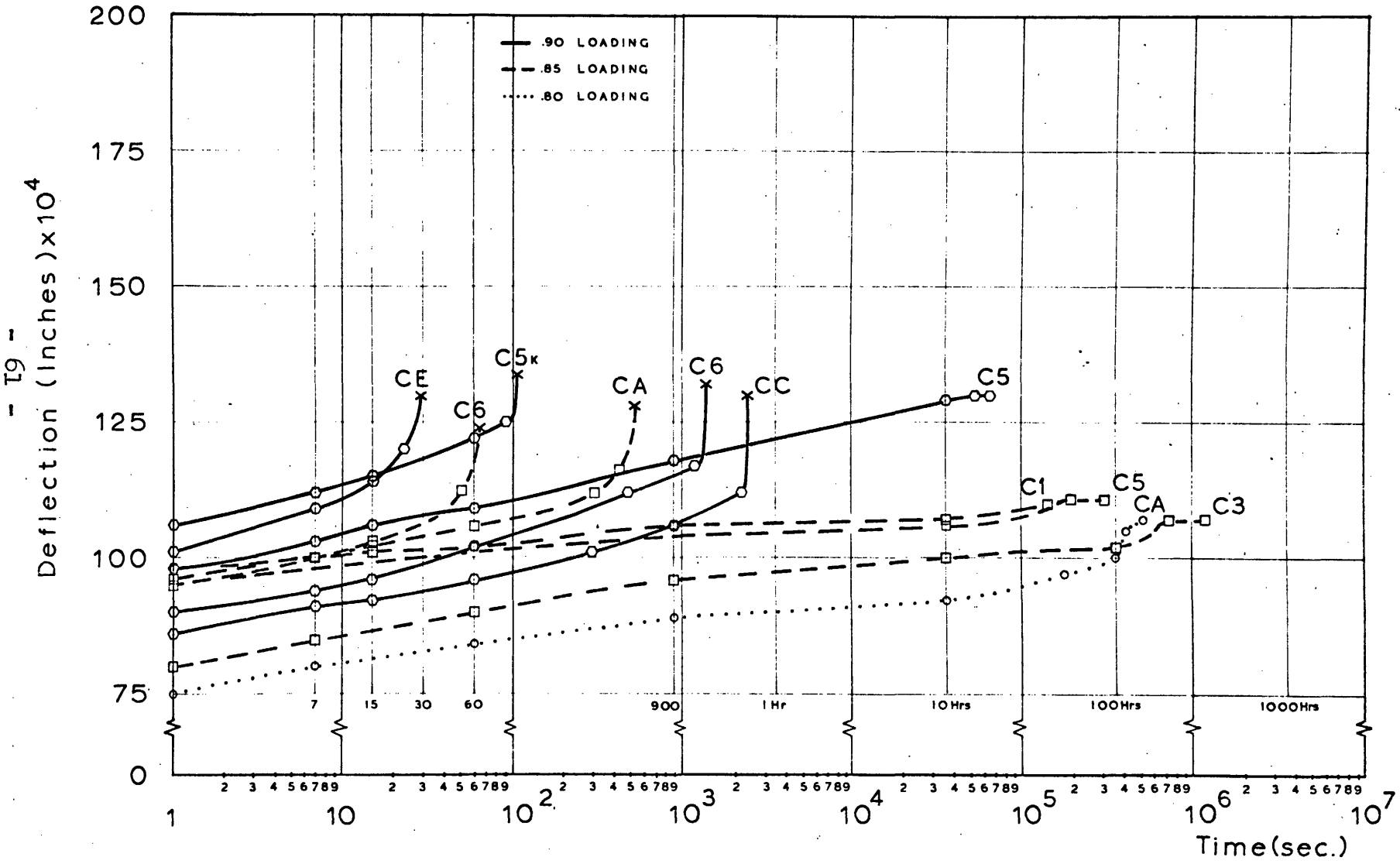

specimens tested at any given load level. This trend was also observed in mortar and concrete specimens tested.

Each mix experienced a sharp increase of creep rate between the .85 and .90 load levels. The propagation of microcracks is felt to be the primary mechanism responsible for the "abrupt" change in creep rate. The growth and coalescence of the microcracks lead to failure of the specimens.

Comparing the creep rates of the three mixes, cement and concrete mixes exhibit, apart from tertiary creep, the same creep rate for a given load level. The creep rates for mortar are, however, higher than the other two mixes for the same load levels. Here it should be remembered that comparable load levels do not mean the same load is applied. This is why the second method of comparison is used.

If the creep rate data were normalized, the creep rate of paste would be the largest and the creep rates of both mortar and concrete would be approximately the same. This may be due to the fact that the mortar and concrete mixes contained the same amount of aggregate (solid concentrations in the two mixes were the same).

Magnitude of Creep: The magnitude of creep or the total time-dependent deformation of the beams depended

strongly on two factors:

1) whether or not failure occurred,

2) whether or not creep arrests were recorded.

Creep arrest is defined as when there is no noticeable increase of deflection for a period of fifty hours or more.

Figure 11 shows that no creep arrests were recorded for the cement paste; whereas, for a comparable time period both mortar and concrete exhibited creep arrests (see Figures 12 and 13). Also there was a tendency for earlier creep arrest with increasing aggregate size. Therefore, the magnitude of creep decreases with increase of aggregate size.

Tertiary Creep Stage: As mentioned in the fracture mechanics discussion, the failure of cement paste is unstable. This fact is confirmed by the near absence of a tertiary creep stage. Impending failure was not signaled by an increase of creep rate on the chart recordings. The two other mixes however showed well defined tertiary creep stages. The aggregates in these mixes inhibit and arrest microcrack propagation and through the mechanism of multiplicity of cracks, increase the effective surface energy necessary for failure. Although the tertiary creep stages of mortar and concrete are much longer than those of paste,

their total duration is still only a matter of seconds.

Thus recognition of impending failure based on tertiary creep rate data would not provide sufficient time for corrective action. A more adequate method would perhaps be based on the time to reach a critical deflection that must not be exceeded [1].

Deflections at Failure: The unstable nature of cement paste is evidenced by the scatter of initial and failure deflections recorded for beams that failed.

The similar scatter in the initial deflections was recorded for observed tests on concrete beams. However, the failure deflections for concrete were fairly uniform and approximately of the same value. This fact would allow the application of a failure criteria based on reaching a critical deflection [1].

The deflections at failure for mortar beams were also fairly uniform; however, they were the highest of the three materials tested. The range of deflections for the various load levels employed covers a wider span in the chart. There seems to be a compromise between the increase of strength due to the addition of the sand to the cement paste and the increase of stiffness exhibited by the beams (the incremental change in strength is larger than the associated change in stiffness, thus providing larger

initial deformation).

The examination of Figure 12 shows that the mortar mix exhibits distinct deflections at each load level. More tests would be needed to comfirm this observation, but if found true it would then be appropriate to apply the failure criterion based on the time to reach a critical deflection that must not be exceeded [1].

Effects of Static Fatigue on Short Time Tests: When sufficient data was obtained from the long term loading in the creep to rupture devices, the beams that had not failed were tested to failure in the Instron Machine.

The load-deflection curves of these tests were then compared with the twenty-eight day load-deflection curves of the same batch with emphasis on the following two points:

1) The failure loads of the beams broken after long term loading were compared with the "average" failure load at twenty-eight days.

2) The average slope of the load-deflection curves taken as the ratio of failure deflection. The ultimate load was also compared with that of the specimens tested at twenty-eight days. This ratio was termed the "stiffness" of the beams (δ/lb) and has the units (in/lb).

The short term failure loads of the beams after having been subjected to static load show the following trends. Both mortar and concrete show approximately the same increase in strength for each load level. This increase is approximately 10% for the .85 load level and 5% for the .80 load level. Paste, however, did not show these trends but showed a slight decrease in strength after loading. The results of these tests are presented in Tables 9, 10 and 11 in the form of "final" load levels (numbers in parentheses). The "final" load level is the ratio of load at which the creep to rupture test was performed to final failure load.

The second point of comparison was the stiffness of the beams before and after the creep to rupture testing. The deflection per pound of loading (δ/lb) was calculated from the load-deflection curves and compared with the one obtained from the instantaneous deformation recorded on the application of the load in creep to rupture. Generally, the correspondence was good, but variations of up to 20% from the mean were recorded. The mean values are 2.14×10^{-4} in/lb for paste, 1.57×10^{-4} in/lb for mortar and 1.34×10^{-4} in/lb for concrete. This confirms the trend of increased stiffness (lower δ/lb) with increased size of the aggregate as noted for the unnotched beams

Table 9

Cement Paste Beams Tested
in Creep to Rupture Device with Clock

Beam	Cast	Load (lbs)	Initial Load Level	(Final)	Length of test (hrs)	Failure
P2	Sept. 7	42.4	.80		204.3	no
P3	Sept. 7	42.4	.80	(.81)	1482	no
PA	Sept. 7	42.4	.80	(.81)	1482	no
PC	Aug. 15	43.4	.85	(.88)	497.5	no
PD	Aug. 15	43.4	.85	(.88)	497	no
PB	Sept. 7	45.1	.85		86.5	yes
P4	Sept. 7	45.1	.85	(.84)	497	no
PD	Sept. 7	45.1	.85		70.3	yes
PD	Jul. 31	48.3	.90		136	accidental
PA	Aug. 1	48.3	.90		161.3	accidental

Dates of casting permit differentiation of batches.

Table 10

Mortar Beams Tested
in Creep to Rupture Device with Clock

Beam	Cast	Load (lbs)	Initial	(Final) Load Level	Length of test (hrs)	Failure
MD	Jul. 24	68.5	.70	(.73)	107.2	no
MF	Jul. 24	68.5	.70	(.71)	107	no
M1	Nov. 7	70.5	.80	(.76)	820	no
M2	Nov. 7	70.5	.80	(.76)	840	no
M5	Nov. 7	70.5	.80	(.74)	840	no
MB	Jul. 29	72.5	.85	(.68)	352.5	no
MC	Jul. 29	72.5	.85	(.78)	352.5	no
MA	Jul. 29	76.5	.90	(.80)	353.5	no
MB	Jul. 24	88.0	.90		120 secs	yes

Dates of casting permit differentiation of batches.

Table 11

Concrete Beams Tested
in Creep to Rupture Device with Clock

Beam	Cast	Load (lbs)	Initial(Final) Load Level		Length of test (hrs)	Failure
C2*	Sept. 26	65.3	.80	(.74)	1800	no
C4*	Sept. 26	65.3	.80	(.78)	1800	no
CF*	Sept. 26	65.3	.80	(.80)	1800	no
CA	Aug. 10	71.0	.85		.15 (540 secs)	yes
CB	Aug. 10	71.0	.85	(.75)	618	no
CC	Aug. 10	71.0	.85	(.78)	562	no
C1*	Sept. 26	69.4	.85	(.75)	480	no
CB*	Sept. 26	69.4	.85	(.77)	480	no
CE*	Oct. 18	65.0	.85	(.71)	1270	
CF*	Oct. 18	65.0	.85		226	yes
CE	Jul. 29	75.1	.90		20 secs	yes
CF	Jul. 29	75.1	.90		618	no

* Was initially loaded for one hour on recording device.

Dates of casting permit differentiation of batches.

(see Table 6). However the increase of stiffness is higher between mortar and concrete for notched specimens than the unnotched beams. This may be due to the fact that relative size of the aggregate as compared to the cross-section area is more pronounced in the notched beam than in the unnotched one.

After the long term loading the beams still showed the same trends of increased stiffness with increase of aggregate size but to a different degree.

The cement paste beams had a general tendency to be less stiff than the beams tested at twenty-eight days, which can be explained by the failure mechanism suggested by Lloyd, Lott and Kesler [16].

This mechanism at a microscopic level is related to the interaction of the primary and secondary bonds present in the paste structure. Upon application of load to a specimen some secondary bonds would tend to fail but the primary bonds which are at least an order of magnitude stronger hold the structure together. It is thought that it is the failure of the secondary bonds that accounts for the decrease in stiffness and decrease in strength recorded for the cement paste beams.

The mortar beams showed no trend of increase or decrease of stiffness after being subjected to static load. The concrete beams, however, did show a slight increase of

stiffness.

In either case it can be noted that the stiffness of the beams is weakened by load when compared to the natural increase of modulus of elasticity with time that was recorded for the mixes in both tension and compression (Figures 9 and 10).

Finally when the results of all the tests run in the creep to rupture devices are tabulated and plotted with load level vs. time to rupture the following trends are apparent (see Figures 14, 15 and 16).

No beam failures were recorded for the beams loaded at an initial load level of .80 for the test times considered. All failures recorded at the .85 load level occurred before the sixth decade (12 days).

Apart from accidental failures all failures occurred in a "triangle" delineated by the .85 load level and a line from 1.0 load level to the intersection of the sixth decade and the .85 load level as shown in Figures 14, 15 and 16..

If a linear relationship (on log scale) between time to failure and load level is assumed, it would take eight decades or approximately 3.2 years of loading to record all the failures (if any) at the .8 load level.

Apparently the increase of strength recorded at this load level (5%) would decrease the probability of failure

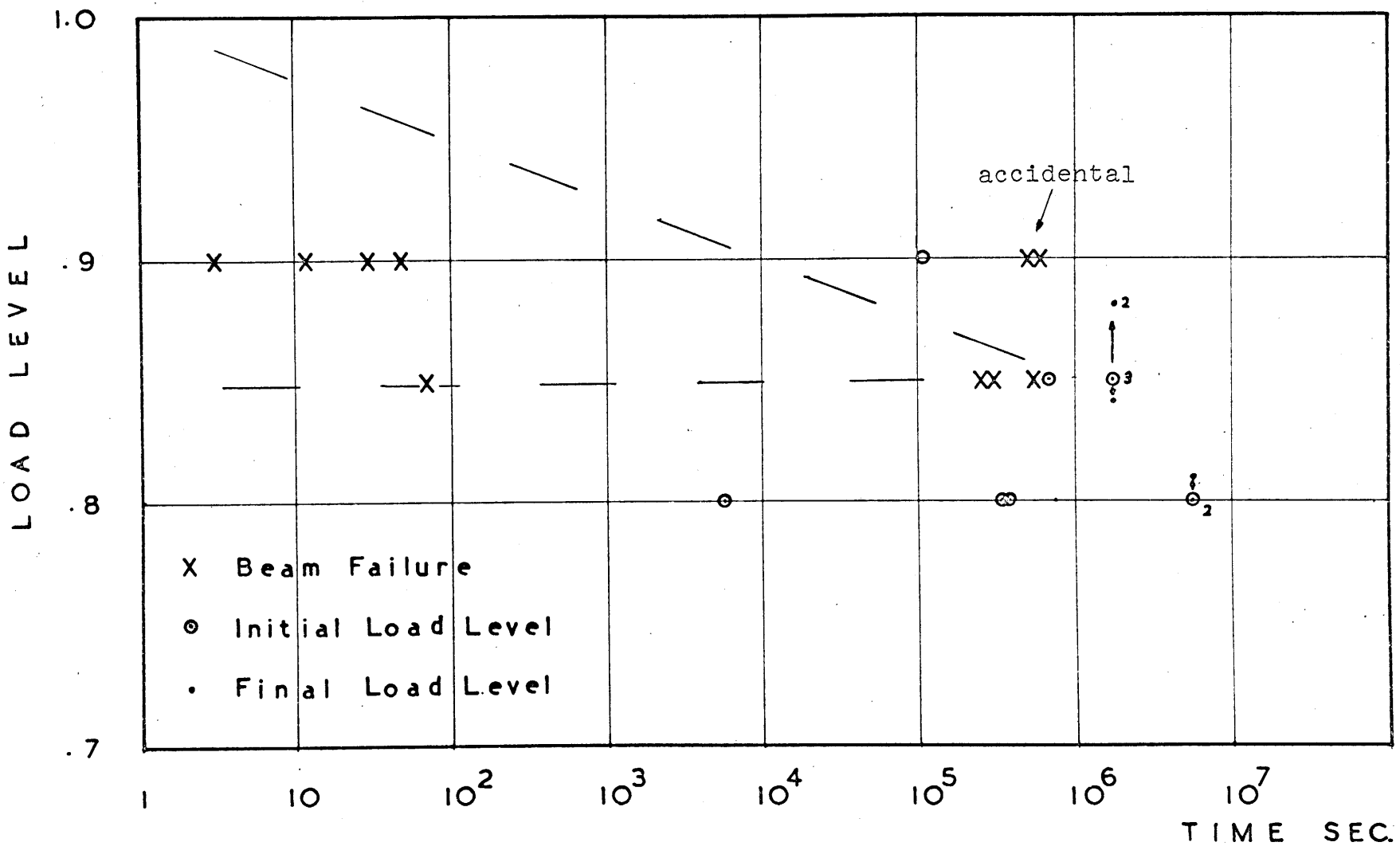

Figure 14. Summary of Tests for Cement Paste. Load Level vs. Time to Rupture or Duration of Test.

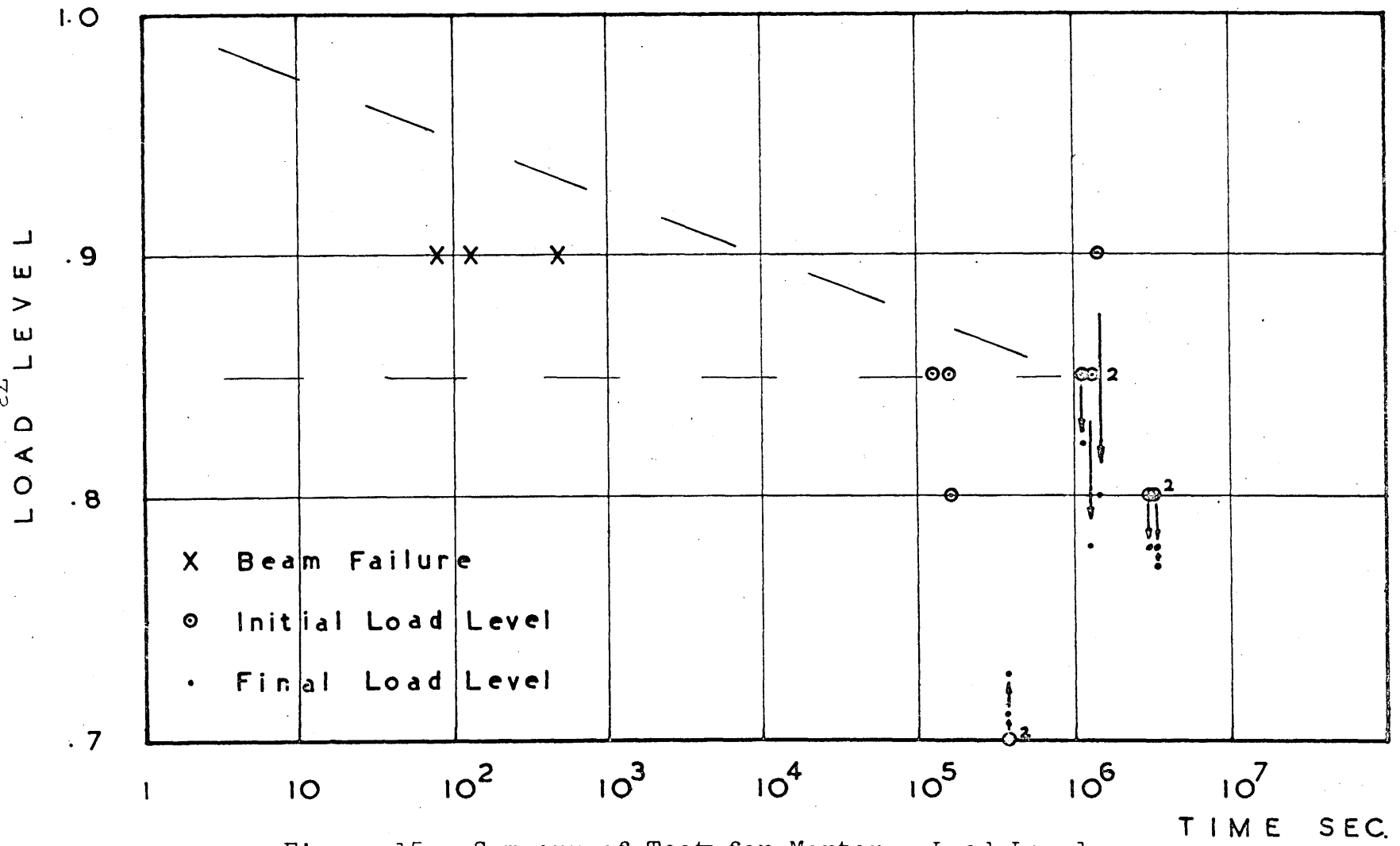

Figure 15. Summary of Tests for Mortar. Load Level vs. Time to Rupture or Duration of Test.

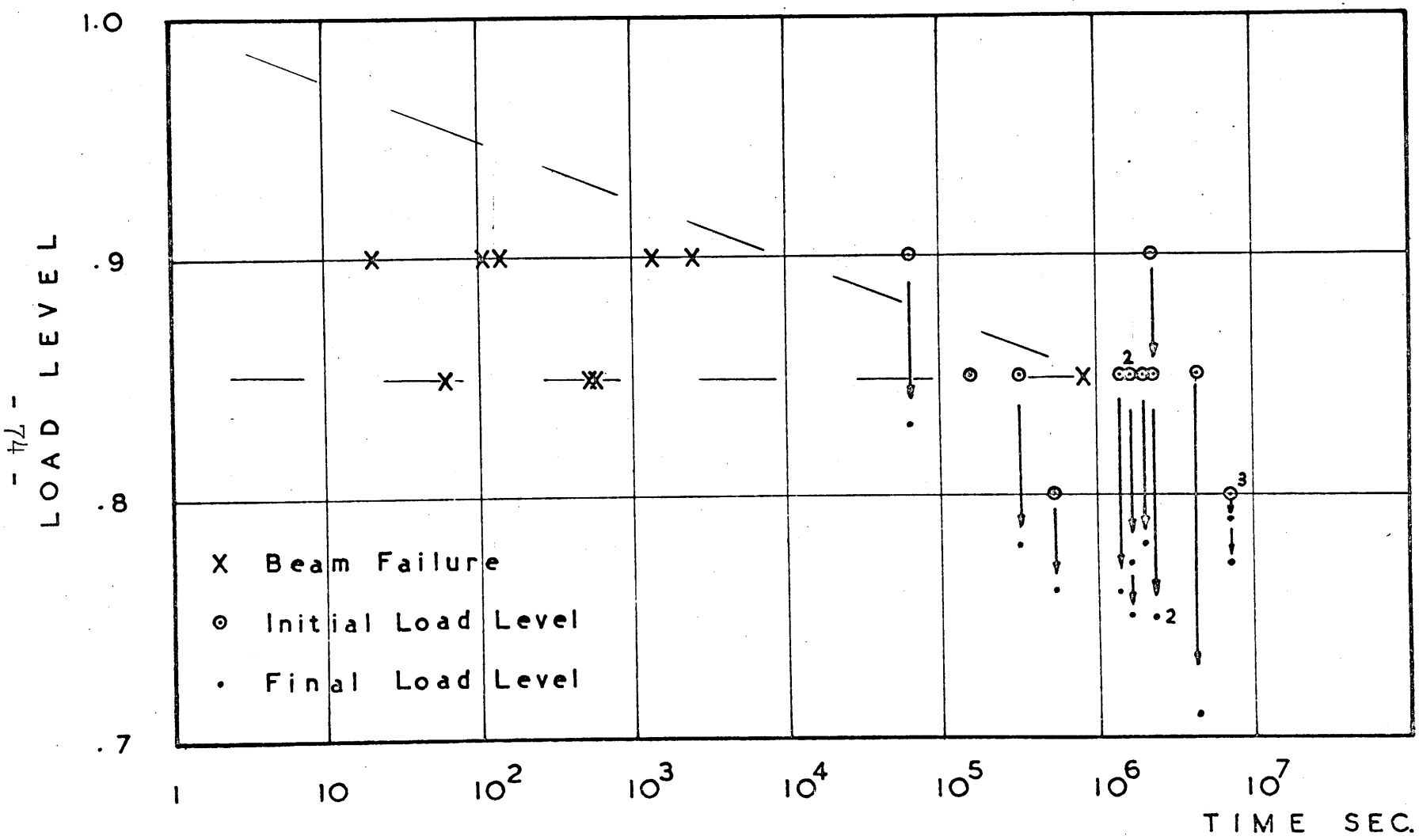

Figure 16. Summary of Tests for Concrete. Load Level vs. Time to Rupture or Duration of Test.

occurring.

So it can safely be said that the mixes studied here, and concrete in particular, would not fail under loadings of up to .80 of the short time ultimate.

This load level is slightly higher than the generally accepted limit of .70-.75 of the short time ultimate mentioned by researchers [14,32,33]. An explanation for this small discrepancy may lie in the following facts.

The ultimate was determined at a slow cross head rate (.005 in/min). Had it been determined at the higher cross head rate ASTM allows (.05 in/min) its value may have been 5% higher. The actual loads at the load levels tested would represent load levels 5% lower, i.e. .75, .80 and .85.

The beams were in an "ideal" environment and not subjected to air drying with subsequent shrinkage cracks. It would have been practically impossible to compare the cement paste beams to the other two mixes if they had been left to dry in the laboratory environment. This was attempted but the shrinkage cracks developed in the cement paste beams generally fractured the specimens.

V. CONCLUSIONS

A series of different experiments were conducted on cement paste, mortar and concrete beams to study what role solid inclusions play in the strengthening and toughening of concrete when subjected to short and long term loading.

The behavior of these three mixes subjected to long term loading approaching the ultimate strength indicated the following trends:

1) Time to failure decreased as the load level increased.

2) All failures at a load level were recorded before a certain maximum time for that load level.

3) There seemed to be a linear relationship (on a semi log scale) between the maximum time to failure and the load level tested.

4) The highest load level at which no failures were recorded was .80 of the short time ultimate.

5) The total time dependent deformation (magnitude of creep) decreased as the size of aggregate was changed from sand to gravel. This is believed to be due to the fact that creep arrests could be achieved sooner with the larger aggregate size mixes.

6) At comparable load levels the creep rate was approximately the same for all three mixes. If normalized to a creep rate per pound of loading this was no longer true.

7) The effects of long term loading on the stiffness of the notched beams; cement paste showed a slight decrease, mortar showed no noticeable effects and concrete showed a slight increase of stiffness compared to that recorded at twenty-eight days.

REFERENCES

1. American Society for Testing and Materials (ASTM) Standards, "Definitions Relating to Methods of Testing," ASTM Designation E 6-61, Sections 64, 65; 1961.

2. Tetelman, A.S. and McEvily Jr., A.J., Fracture of Structural Materials, John Wiley and Sons, Inc., New York, 1967.

3. Richards, C.W., Engineering Materials Sciences, Wadsworth Publishing Co., Inc., Belmont, California, 1961.

4. Low Jr., J.R., Fracture of Solids, Interscience, New York, 1963, pp. 197.

5. Garofalo, F., Domis, W. and Gemminger, F., Transactions of the American Institute of Mining Engineers (AIME) 230, 1460; 1964.

6. Garofalo, F., Fundamentals of Creep and Creep Rupture, Macmillan, New York, 1965.

7. Cottrell, A.H., The Mechanical Properties of Matter, John Wiley and Sons, Inc., New York, 1964.

8. Moffatt, W.G., Pearsall, G.W. and Wulff, J., The Structure and Properties of Materials: Vol. I, Structure, John Wiley and Sons, Inc., New York, 1964.

9. Hayden, H.W., Moffatt, W.G. and Wulff, J., The Structure and Properties of Materials: Vol. III, Mechanical Behavior, John Wiley and Sons, Inc., New York, 1965.

10. Broutman, L.J. and Krock, R.H., Modern Composite Materials, Addison-Wesley Publishing Co., Reading, Massachusetts, 1967.

11. Curran, R.J., "Dead Load Creep Rupture of Poly Methyl Methacrylate," Research Report R63-55, Department of Civil Engineering, Massachusetts Institute of Technology, December 1963.

12. Nielson, L.E., Mechanical Properties of Polymers, Reinhold Publishing Corp., New York, 1965.

13. Baer, E., Engineering Design for Plastics, Polymer Science and Engineering Series (SPE), Reinhold Publishing Corp., New York, 1964.

14. Winter, G., O'Rourke, C.E., Nilson, A.H. and Urquhart, L.C., Design of Concrete Structures, McGraw-Hill, New York, 1964.

15. Neal, J.A., Kung, S.H.C. and Kesler, C.E., "Third Progress Report on Mechanism of Fatigue Failure in Concrete," T. & A.M. Report No. 623, University of Illinois, 1963.

16. Lloyd, J.P., Lott, J.L. and Kesler, C.E., "Fatigue of Concrete," T. & A.M. Report No. 675, University of Illinois, 1967.

17. Philleo, R.E., "Elastic Properties and Creep of Hardened Concrete," in Concrete and Concrete Making Materials, ASTM Publication ST 169-A.

18. Washa, G.W., "Comparison of the Physical and Mechanical Properties of Hand-Rodded and Vibrated Concrete Made with Different Cements," American Concrete Institute (ACI) Proceedings, Vol. 36, 1940, pps. 617-648.

19. Troxell, G.E. and Davis, H.E., Composition and Properties of Concrete, McGraw-Hill, New York, 1956.

20. Troxell, G.E., Davis, H.E. and Kelly, J.W., Composition and Properties of Concrete, Second Edition, McGraw-Hill, New York, 1968.

21. Lorman, W.R., "Theory of Concrete Creep," ASTM Proceedings, Vol. 40, 1940, pps. 1082-1102.

22. Hansen, T.C., "Creep of Concrete," Swedish Cement and Concrete Research Institute, Royal Institute of Technology, 1958.

23. Freyssinet, E., "The Deformation of Concrete," Magazine of Concrete Research, Vol. 3, No. 8, December 1951, pps. 49-56.

24. Mullen, W.G. and Dolchi, W.G., "Creep of Portland-Cement Paste," ACI Proceedings, Vol. 64, 1964, pps. 1146-1171.

25. Freudenthal, A.M. and Roll, F., "Creep and Creep-Recovery of Concrete Under High Compressive Stress," Journal of the ACI, June 1968, pps. 1111-1142.

26. Davis, R.E., Davis, H.E. and Brown, E.H., "Plastic Flow and Volume Changes of Concrete," ASTM Proceedings, Vol. 37, Part II, 1937, pp. 317.

27. Dong, R.G., "A Functional Cumulative Damage Theory and its Relation to two Well-Known Theories," (Palm-Langer-Miner Theory and Williams Theory), University of California, January 1967.

28. Glanville, W.H., "The Creep or Flow of Concrete Under Load," Building Research Technical Paper No. 12, Department of Scientific and Industrial Research, London, 1930.

29. Ross, A.D., "Creep of Concrete Under Variable Stress," ACI Proceedings, March 1958, pps. 739-758.

30. Fluck, P.G. and Washa, G.W., "Creep of Plain and Reinforced Concrete," ACI Proceedings, April 1958, pps. 879-896.

31. Glanville, W.H. and Thomas, F.G., "Further Investigations on the Creep or Flow of Concrete Under Load," Building Research Technical Paper No. 21, 1939.

32. Sell, R., "Investigation into Strength of Concrete Under Sustained Loads," RILEM Bulletin No. 5, 1959.

33. Hansen, T.C., "Cracking and Fracture of Concrete and Cement Paste," in Causes, Mechanism and Control of Cracking in Concrete, ACI Publication SP-20, 1968.

34. Leslie, J.R. and Cheesman, W.J., "An Ultrasonic Method of Studying Deterioration or Cracking in Concrete Structures," ACI Proceedings, Vol. 46, 1950, pps. 17-36.

35. Shah, S.P. and Chandra, S., "Critical Stress, Volume Change and Microcracking of Concrete," ACI Proceedings, September 1968, pps. 770-780.

36. Rusch, H., "Physical Problems in Testing Concrete," Zement-Kolk-Grips, Vol. 12, No. 1, January 1959, Library Transaction No. 86, Cement and Concrete Association, London.

37. Bieniawski, Z.T., "Mechanisms of Brittle Fracture of Rock," CSIR Report MEG 580, National Mechanical Engineering Research Institute, Pretoria, South Africa, 1967.

38. Bieniawski, Z.T., "Mechanisms of Brittle Fracture of Rock": Part III, "Fracture in Tension and Under Long Term Loading," International Journal of Rock Mechanics and Mining Sciences, 1967.

39. Kaplan, M.F., "Crack Propagation and Fracture of Concrete," Journal of the ACI, Vol. 58, No. 5, November 1961, pps. 591-610.

40. ASTM Standards, "Standard Method of Test for Sieve Analysis of Fine and Coarse Aggregates," ASTM Designation C 136.

41. ASTM Standards, "Standard Method of Test for Measuring Mortar-Making Properties of Fine Aggregate," ASTM Designation C 87.

42. ASTM Standards, "Standard Method of Test for Flexural Strength of Concrete Using Simple Beam with Center-Point Loading," ASTM Designation C 293-59. (calculation of the modulus of rupture)

43. ASTM Standards, "Standard Method of Test for Compressive Strength of Molded Concrete Cylinders," ASTM Designation C 39.

44. Walker, S. and Bloem, D.L., "Effects of Aggregate Size on Properties of Concrete," ACI Proceedings, Vol. 57, 1960-1961, pps. 283-298.

45. Ishai, O., "Influence of Sand Concentration and Deformations of Mortar Beams Under Low Stress," ACI Proceedings, Vol. 58, No. 5, 1961-1962, pps. 611-623.

46. Moavenzadeh, F., Kuguel, R. and Keat, L.B., "Fracture of Concrete," Research Report R68-5, Department of Civil Engineering, Massachusetts Institute of Technology, March 15, 1968.

47. Brown Jr., W.F. and Strawley, J.E., Plain Strain Crack Toughness Testing of High Strength Metallic Materials, ASTM Publication, 1966. (Library of Congress Catalog Card Number 66-29517)

48. Lott, G.L. and Kesler, C.E., "Crack Propagation in Plain Concrete," T. & A.M. Report No. 648, University of Illinois, 1964.

49. Irwin, G.R., Journal of Applied Mechanics, Vol. 61, pp. 49, 1939.

50. Nakayama, T., "Direct Measurement of Fracture Energies of Brittle Heterogeneous Materials," Journal of the American Ceramic Society, 1965.

51. Bremner, T., Unpublished work done at the Materials Laboratory, Department of Civil Engineering, Massachusetts Institute of Technology, 1968.

52. Hsu, T.T.C., Slate, F.O., Sturman, G.M. and Winter, G., "Microcracking of Plain Concrete and the Shape of the Stress-Strain Curve," ACI Proceedings, Vol. 60, 1963, pps. 209-224.

53. Glucklich, J., "The Influence of Sustained Loads on the Strength of Concrete," RILEM Bulletin No. 5, December 1959, pps. 14-17.

54. Hughes, B.P. and Chapman, G.P., "The Deformation of Concrete and Microcracking in Compression or Tension with Particular Reference to Aggregate Size," Magazine of Concrete Research, Vol. 18, No. 54, March 1966, pps. 19-24.

55. Welch, G.B., "Tensile Strains in Unreinforced Concrete Beams," Magazine of Concrete Research, Vol. 18, No. 54, March 1966.

Appendix A

List of Abbreviations in Text

(in alphabetic order)

A	aggregate
a	notch depth (inches)
C	concrete
c	cement
cm	centimeter (0.01 meter)
d	beam depth (inches)
E	modulus of elasticity
ft	foot (12 inches)
g	gram (.001 kilo)
G_c	critical strain energy release rate ($in \cdot lb/in^2$)
in	inch
K_c	critical stress intensity factor ($lb \cdot in^{-3/2}$)
L	length of beam (inches)
lb	pound
M	mortar
P	paste (cement)
PMMA	poly methyl methacrylate (polymer)
psi	pounds per square inch (lb/in^2)
	one-half of grain diameter
S	span of testing (inches)
S-N	stress vs. number of cycles (fatigue)
SSD	saturated surface dry
T	time

t	service life
TM	absolute melting temperature (°K)
V	creep rate
W	water
w	beam width (inches)
γ_{eff}	effective surface energy
γ_G	specific surface energy calculated from Irwin's expression $\pi K_c^2/2E$
δ	deflection of beam
δ/lb	deflection per pound of loading (in/lb)
	measure of stiffness of notched beams
ε	strain
σ	stress (lb/in^2)

Appendix B

List of Deflections Recorded in Creep to Rupture Curves

(Figures 11, 12, 13)

Beam	PE*	PF*	PB*	PC*	PF
Cast	Sept. 7	Sept. 7	Jul. 31	Jul. 31	Jul. 31
Load (lbs)	47.7	47.7	48.3	48.3	48.3
Load Level	.90	.90	.90	.90	.90
Initial Deflection	98	86	106	117	98
7 secs	3 secs 104	6 secs 93	113	126	105
15 secs		12 secs 96	116	25 secs 135	109
60 secs			41 secs 120	30 secs 138	111
900 secs			47 secs 125		115
36000 secs					128
360000 secs					104000 133

* Beam failed under this load.

Beam	PE*	PD*	P4	PB
Cast	Aug. 13	Sept. 7	Sept. 7	Nov. 19
Load (lbs)	43.4	45.1	45.1	49.0
Load Level	.85	.85	.85	.85
Initial Deflection	116	100	91	93
7 secs	124	103	94	93
15 secs		104		96
60 secs	127	107	97	97
900 secs	131	69 secs 109	101	102
36000 secs	137		108	106
360000 secs	158		129	120
	580000 178		670000 135	1120000 126

* Beam failed under this load.

Beam	PC	PB	PE
Cast	Aug. 1	Aug. 15	Nov. 21
Load (lbs)	43.0	40.8	48.0
Load Level	.80	.80	.80
Initial Deflection	93	95	78
7 secs	103	98	82
15 secs		99	83
60 secs	106	101	84
900 secs	110	106	88
36000 secs	116	5820 112	94
360000 secs	324000 133		100

Beam	MF*	MD*	MA	MB	MC
Cast	Jul. 24	Jul. 24	Aug. 5	Aug. 5	Aug. 5
Load (lbs)	88.0	88.0	68.7	68.7	64.0
Load Level	.90	.90	.85	.85	.80
Initial Deflection	135	132	123	118	118
7 secs	154	144	126	123	122
15 secs	156	148			
60 secs	61 secs 166	155	133	128	127
900 secs	75 secs 178	393 secs 166	138	137	132
36000 secs		456 183	146	139	140
360000 secs			113000 149	160000 142	174000 143

* Beam failed under this load.

Beam	MC	M2	M5	MC
Cast	Nov. 7	Nov. 7	Nov. 7	Aug. 5 Retest
Load (lbs)	70.5	70.5	70.5	78.0
Load Level	.80	.80	.80	.85 (.82) 46 days
Initial Deflection	90	104	88	126
7 secs	95	108	92	132
15 secs	97	110	93	
60 secs	102	114	96	134
900 secs	111	121	103	139
36000 secs		3000 124	3600 105	148
360000 secs	128	8400 126	6300 107	170
	540000 129	continued on other loading frame		900000 193
	720000 130			1113000 193
	1240000 130			

Beam	CE*	C5	C6*	CC*	C5K*
Cast	Sept. 26	Sept. 26	Oct. 18	Oct. 18	Oct. 18
Load (lbs)	73.5	73.5	69.0	69.0	69.0
Load Level	.90	.90 (.83)	.90	.90	.90
Initial Deflection	101	98	90	86	106
7 secs	109	103	94	91	112
15 secs	114	106	96	92	115
60 secs	23 secs 120	109	102	96	122
900 secs	29 secs 130	118	240 secs 108	106	90 secs 125
36000 secs		129	480 112	2280 112	105 secs 134
360000 secs		54000 130	1200 118	2450 130	
		64800 130	1375 132		

* Beam failed under this load.

Beam	C3	CA*	C6*	C1
Cast	Oct. 18	Sept. 26	Sept. 26	Sept. 26
Load (lbs)	66.5	69.4	69.4	69.4
Load Level	.85 (.76)	.85	.85	.85
Initial Deflection	80	98	95	96
7 secs	85	100	100	100
15 secs		102	103	101
60 secs	90	106	50 secs 112	102
900 secs	96	300 secs 112	64 secs 124	106
36000 secs	100	480 secs 120		107
360000 secs	102	525 secs 128		144000 110
	720000 107			
	1200000 107			

* Beam failed under this load.

Beam	C5	CA
Cast	Sept. 26 Retest	Oct. 13
Load (lbs)	69.4	61.1
Load Level	.85 (.78)	.80 (.76)
Initial Deflection	95	75
7 secs	98	80
15 secs		
60 secs	101	84
900 secs	104	89
36000 secs	106	92
360000 secs	180000 110	100
	198000 111	415000 105
	306000 111	505000 107